2018

PREDICTING 100-YEAR STORM WAVE'S RUNUP FOR THE COAST OF RHODE ISLAND USING A FULLY NONLINEAR MODEL

Gregory Westcott
University of Rhode Island, gwestcott@my.uri.edu

PREDICTING 100-YEAR STORM WAVE'S RUNUP FOR THE COAST OF RHODE ISLAND USING A FULLY NONLINEAR MODEL

BY

GREGORY J. WESTCOTT

A THESIS SUBMITTED IN PARTIAL FULFILLMENT OF THE

REQUIREMENTS FOR THE DEGREE OF

MASTER OF SCIENCE

IN

OCEAN ENGINEERING

UNIVERSITY OF RHODE ISLAND

2018

MASTER OF SCIENCE THESIS

OF

GREGORY J. WESTCOTT

APPROVED:

Thesis Committee:

Major Professor Annette R. Grilli

Stéphan T. Grilli

Tetsu Hara

M Reza Hashemi

Nasser H. Zawia

DEAN OF THE GRADUATE SCHOOL

UNIVERSITY OF RHODE ISLAND

2018

ABSTRACT

A phase resolving model (FUNWAVE) is used to simulate the 100-year storm. Results are compared to those of the FEMA approved phase averaged model STWAVE, allowing for a direct comparison of water elevations along the coast of Narragansett R.I. Effects of sediment erosion/deposition are taken into consideration using the model XBeach to predict changes to the coastline, which are then used in FUNWAVE's grid to model wave runup. The test site for this study is Narragansett Town Beach (R.I) and the surrounding infrastructure in the area. Results show a significant amount of beach erosion/deposition along the Town Beach, but not much elsewhere as it is mostly rocky coastline protected by a seawall. Comparisons of significant wave heights predicted by STWAVE and FUNWAVE show a stark difference with much higher values predicted by the phase resolving model FUNWAVE. This increase in wave height results from dynamic wave setup, which is not modeled the phase-averaged model STWAVE. Empirical calculations for wave runup (Stockdon et. al., 2012) compare very well to FUNWAVE's results, while STWAVE clearly underpredicts runup. Impulse forces calculated along the coastline greatly increase when sediment erosion is considered, with much higher values occurring in the nearshore area of the eroded coastline. Differences in the predicted wave heights between the simulations performed in this study show the importance of using a phase resolving wave model, which is the only way to include the additional effects of dynamic wave runup.

ACKNOWLEDGMENTS

I would like to express the sincerest gratitude to my advisor Dr. Annette Grilli for her continuous support of my M.S. study and related research, for her patience, motivation, and immense knowledge. Her guidance truly helped me with all of the research and writing of this thesis. I could not have imagined having a better advisor and mentor for my M.S. study.

Along with my advisor, I would like to thank the rest of my thesis committee: Dr. Stéphan Grilli, Dr. M Reza Hashemi, Dr. Tetsu Hara, Dr. Christopher Baxter, and Dr. Peter Cornillon for their time and help through out the entire graduate school process. The example that you set for students and the University is prolific, and your teachings constantly inspired me to be the best possible student that I could be.

I would like to thank my officemates, Lauren, Pat, Chris, and Fatima for their continuous help and insight into a multitude of roadblocks and challenges.

Last but not least, I would like to thank my family: my Mom, Gözde, Jess, Jenn, and Rae for their constant support at home and with life in general, with out you this process would not have been the same.

PREFACE

For the purpose of this work the manuscript format is in use, containing one manuscript entitled "Predicting 100-year Storm Wave's Run-up for the Coast of Rhode Island using a Fully Nonlinear Model" and is in preparation for submission to JOURNAL.

TABLE OF CONTENTS

ABSTRACT . . . ii

ACKNOWLEDGMENTS . . . iii

PREFACE . . . iv

TABLE OF CONTENTS . . . v

LIST OF FIGURES . . . vii

LIST OF TABLES . . . xi

MANUSCRIPT

1 Predicting 100-year Storm Wave's Run-up for the Coast of Rhode Island using a Fully Nonlinear Model . . . 1

1.1 Introduction . . . 2

1.1.1 *Objective* . . . 6

1.1.2 *Test site* . . . 6

1.2 Data . . . 7

1.3 Methodology . . . 9

1.3.1 *Shoreline morphology during 100-Year storm: modeling dune erosion* . . . 10

1.3.2 *Modeling inundation using phase-averaged wave model* . . . 13

1.3.3 *Modeling inundation using phase-resolving wave model* . . . 16

1.4 Results . . . 20

1.4.1 *Dune erosion* . . . 20

1.4.2 *Nested grid boundary conditions* . . . 20

Page

1.4.3 *Inundation using FUNWAVE* 23

1.4.4 *Runup at critical save points* 30

1.5 Conclusion 35

List of References 37

APPENDIX

Appendix 40

A.1 XBeach Params.txt 40

A.2 STWAVE Grid Schematic 41

A.3 FUNWAVE: Obstacle File 41

A.4 FUNWAVE: Breakwater File 42

A.5 FUNWAVE: Input File *input.txt* 42

A.6 STWAVE Results Narragansett Bay 47

A.7 FUNWAVE: Irregular Wavemaker 47

A.8 FUNWAVE: Wavemaker Timeseries 49

A.9 FUNWAVE scenario two: Irregular Wavemaker Validation 51

A.10 Stockdon Wave runup definitions 51

A.11 Stockdon beach slope definitions 51

A.12 Impulse force equations 51

BIBLIOGRAPHY 52

LIST OF FIGURES

Figure		Page
1.1	Area of interest outlined for Narragansett Rhode Island.	7
1.2	Elevation map of Study Area, interpolated to 2 meter resolution. Color scale in meters. Data from (Environmental Data Center, 2014).	8
1.3	Friction map of Study Area, defined by Manning Coefficient n (color scale: $s/m^{1/3}$) Data:(RIGIS, 2015).	8
1.4	XBeach Computational Elevation Map defined by NAVD88 datum. Coast line rotated to be aligned along eastern side of grid. (color scale: meters) (Environmental Data Center, 2014).	11
1.5	XBeach Nonerodible Locations (rocks, walls, buildings, roads) (Google, 2018).	12
1.6	NACCS data for storm 4457 in Narragansett Rhode Island (a) Significant Wave height (b) Peak Period (c) Storm Surge (Cialone et al., 2015).	14
1.7	STWAVE grid (large grid) and nested coastal grid (small grid) used to simulate waves for the 100-year storm using NACCS 's spectral parameters in boundary condition on the edge of the large grid. . . .	15
1.8	FUNWAVE Computational Grid (a) DEM elevation map (b) DEM elevation with 3.7 m of surge. The solid line shows the limit of the the 'fake' lateral boundary used for periodic boundary conditions, the stars mark stations that were placed along 3 transects to test the wave maker (top to bottom: T1,T2,T3). Color Scale is in meters. .	17
1.9	FUNWAVE Breakwater locations for the DEM simulation have been highlighted on Google Earth (Google, 2018).	19
1.10	FUNWAVE Obstacle locations have been highlighted on Google Earth (Google, 2018). Obstacle points identify spots on the grid that remain dry (building with foundations).	19
1.11	XBeach results for sediment transport, post storm bathymetry/topography (color scale: meters). The periodicity region has been marked with a solid line.	21

Figure **Page**

1.12 XBeach results for sediment *erosion*, positive values depict a decrease in elevation relative to the original DEM grid, data from (Environmental Data Center, 2014). Contour lines depict original DEM levels spaced at 5 m intervals, the asterisks mark 11 key locations used for model comparisons. Data is displayed on Google Earth (Google, 2018) (color scale: meters). 21

1.13 XBeach results for sediment *deposition*, positive values depict an increase in elevation relative to the original DEM grid, data from (Environmental Data Center, 2014). Contour lines depict original DEM levels spaced at 5 m intervals, the asterisks mark 11 key locations used for model comparisons. Displayed on Google Earth (Google, 2018) (color scale: meters). 22

1.14 STWAVE results for significant wave height (Narragansett Town Beach, R.I). A close up view of results in the area of interest, note that dune tops are 'dry'. Data is displayed on Google Earth (Google, 2018) (color Scale: meters). 23

1.15 Envelope of maximum surface elevations (m) in FUNWAVE simulations (referred to NAVD88) for: (a) scenario 1 (dune intact), (b) scenario 2 (dune eroded). 25

1.16 Difference in maximum surface elevations (m) from FUNWAVE simulations (referred to NAVD88). Eroded > Intact: found by subtracting scenario 1 (dune intact) from scenario 2 (eroded dune). 25

1.17 Maximum flow depths (m) from FUNWAVE simulations for: (a) scenario 1 (dune intact), (b) scenario 2 (eroded dune). 26

1.18 Difference in maximum flow depths (m) from FUNWAVE simulations (referred to NAVD88). Eroded > Intact: found by subtracting scenario 1 (dune intact) from scenario 2 (eroded dune). 26

1.19 Maximum flow depths (m) in the swash zone (above static surge = 3.7 m) from FUNWAVE simulations for: (a) scenario 1 (dune intact), (b) scenario 2 (eroded dune). 27

1.20 Maximum impulse forces (kN/m) at the Dunes Club and eastern end of Narragansett town beach estimated from FUNWAVE simulations for: (a) scenario 1 (dune intact) (b) scenario 2 (eroded dune). 28

Figure **Page**

1.21 Difference in maximum impulse forces (kN/m) at the Dunes Club and eastern end of Narragansett town beach estimated from FUNWAVE by subtracting scenario 1 (dune intact) from scenario 2 (eroded dune). 28

1.22 Maximum impulse forces (kN/m) on Condo's along Narragansett beach from FUNWAVE simulations for: (a) scenario 1 (intact dune), (b) scenario 2 (eroded dune). 29

1.23 Maximum impulse forces (kN/m) on two houses along Narragansett beach from FUNWAVE simulations for: (a) scenario 1 (intact dune), (b) scenario 2 (eroded dune). 29

1.24 Eleven save points are marked by asterisks. The four asterisks with rectangular box's mark locations used for wave runup empirical calculations based on Stockdon et. al. (2006). 30

1.25 Transect locations selected for empirical wave runup calculations as defined by Stockdon et. al. (2012). From left to right, transects 1,2,3, and 4, corresponding to 'save points' (4,5,6, and 8, respectively) in Table 1.11. 33

1.26 Transect data (a) T1, (b) T2, (c) T3, (d) T4. Maximum surface elevations ($\eta_{\max}$) are displayed for FUNWAVE (blue line), and STWAVE (red line), with the original DEM bathymetry/topography (black line). The static surge level = 3.7 m (dashed pink line), and NAVD88 *z=0* (black dashed line). 35

A.1 STWAVE Grid Schematic. 42

A.2 STWAVE results for significant wave height (Narragansett Bay, R.I). The FUNWAVE domain has been outlined, with the three input locations marked as stars along the outer boundary (Table 1.9). Data is displayed on Google Earth (color scale: meters). 48

A.3 Time series of surface elevations (*eta* meters) from Transect one, station 1. Data collected at 0.1 second intervals over a total of 11,000 seconds. 49

A.4 "Sketch defining the relevant morphological and hydrodynamic parameters in the storm impact scaling model of Sallenger (2000) (modified from Stockdon and other, 2009)." (Stockdon et. al., 2012) 50

A.5 "Cross-shore profile of lidar-based elevations indicating the locations of the dune crest (x_c,z_c), toe (x_t,z_t), shoreline (x_{sl},z_{sl}), mean beach slope (β_m), mean high water (MHW), and high water line (HWL). Abbreviation: m, meter." (Stockdon et. al., 2012 51

LIST OF TABLES

Table **Page**

1.1 Manning bottom friction coefficient n ($s/m^{1/3}$) as a function of land type (Arcement and Schneider, 1989). 9

1.2 Summary of the numerical scenarios. 10

1.3 XBeach Grid Parameters; origin(Xo,Yo), grid spacing (Dx/Dy), grid dimension (X Dim/ Y Dim), rotation angle (θ) defined positive in clockwise direction. 11

1.4 Large grid computational domains parameters used for wave propagation with STWAVE: origin (Xo/Yo), grid spacing (Dx/Dy), number of rows (Ni), number of columns (Nj), rotation angle (θ). 14

1.5 STWAVE input parameters as defined by the shallow water TMA spectrum, with the wind speed, wind direction, significant wave height (Hs), peak period (Tp), wave direction (α), and maximum surge. 15

1.6 FUNWAVE Grid Parameters. With its origin (Xo,Yo), grid spacing (Dx/Dy), x- and y-dimensions (mglob/nglob), and rotation angle (θ). 17

1.7 FUNWAVE wave maker grid setup for Narragansett, Rhode Island. 18

1.8 Spectral parameters and initial storm surge level implemented on FUNWAVE irregular wave maker. The frequency range has been defined for incoming wave field based on the peak period (Tp), significant wave height (Hs), and depth. 20

1.9 STWAVE results for spectral parameters; significant wave height (Hs), and peak period (Tp) at three locations along the offshore boundary. 22

1.10 FUNWAVE irregular wave-maker validation: H_{s} and H_{mo} at the three transects, T1,T2,T3 (each, 5 stations (*Sta*)) 100 meters apart (Figure 1.8); calculated using Welch's power density spectrum (*PW*), and the zero-up-crossing method (*ZUC*), respectively. 24

Table **Page**

1.11 Significant wave heights compared at 11 key points for each simulation including STWAVE, FUNWAVE scenario 1 and 2 (*FW* dune intact and eroded, respectively) 31

1.12 Impulse forces, F_i (kN) compared at 11 key locations for FUNWAVE scenario 1 and 2 (dune intact and eroded, respectively) 31

1.13 Wave runup (m) estimated using Stockdon's formulation (Stockdon et. al., 2012) FUNWAVE (dune intact) and STWAVE along 4 transects across Narragansett Town Beach (Figure 1.25). 34

A.1 FUNWAVE irregular wave-maker validation for XBeach post grid simulation. Significant wave heights are presented for three transects (T1,T2,T3) consisting of 5 stations (*Sta*) each separated by 100 meters (visually represented in Figure 1.8). *Hs* values were calculated at each station using both Welch's power density spectrum (*PWelch*), and the zero-up-crossing method (*ZUC*) 50

MANUSCRIPT 1

Predicting 100-year Storm Wave's Run-up for the Coast of Rhode Island using a Fully Nonlinear Model

1.1 Introduction

The impact of storms on coastal communities can be devastating and, with storm intensities potentially on the rise as a result of global climate change (Knutson et al., 2010), it becomes increasingly important to use accurate tools to predict storms potential effects. Today there are numerous wave models used to simulate storm conditions, but many of these use phase-averaged equations to solve for wave action conservation. This approach can be sufficiently accurate while waves are in deeper water, but as waves propagate towards the surf zone many physical aspects will be missed including dynamic wave-setup and run-up. In order to model waves in the surf zone as accurately as possible, we use a phase resolving model the Fully Uncoupled Non-Linear Wave model (FUNWAVE) (Kirby et al., 1998). We attempt to assess the epistemic uncertainty associated with choice of wave model by comparing the inundation levels using both phase-averaged and phase-resolving models. We selected as the test site the small coastal community of Narragansett, Rhode Island (RI) on the U.S. North East Atlantic coastline. A Synthetic 100-year Design Storm (SDS) is selected for this numerical experiment, referred to as the "100-year" storm, or the storms with an annual probability of exceedance of 1%. The SDS is defined based on the North Atlantic Coast Comprehensive Study (NACCS) performed by the U.S. Army Corps of Engineers (USACE), (Cialone et al., 2015; Jensen et al., 2016).

The wave run-up conventionally defined as the time-varying maximum water elevation on the shoreline, about the still-water level, can be split into two components, the static wave set-up (often referred to as "set-up"), a super elevation of the mean water level, and the dynamic wave set-up or swash, a short-time fluctuations about that mean (Longuet-Higgins and Stewart, 1964; Guza and Thornton, 1982; Holman and Sallenger, 1985). The static wave set-up is the additional water elevation relative to the Mean Sea Level (MSL) created from the transfer of momentum to the water column when waves are breaking while the dynamic wave set up or swash results from the "surf-beats" or slow moving (minutes) oscillations of the mean super-elevated water level on the shoreline (Schäffer and Svendsen, 1989; Bender and Dean, 2005). Together the static and dynamic wave set-up, create what is referred to as the maximum wave run-up, or the maximum vertical extent of the wave up-rush (Nielsen and Hanslow, 1991). Generally, the wave run-up is defined as the maximum water level that is exceeded by 2 percent of waves (Battjes, 1974).

Community planning for extreme weather conditions including flooding is essential for proper evacuation routes, property management, and the overall safety of citizens. Along the coast of the United States FEMA has published Flood Insurance Rate Maps (FIRMs) that specify zones of inherent hazard due to flooding as a result of severe storms (FEMA, 2016). Hazard zones are identified by their risk of inundation associated with the annual 1 percent probability of exceedence flood event. Current RI flood maps were developed in 2012 by a consulting firm, the Strategic Alliance for Risk Reduction (STARR), using FEMA's accepted methodology. Thus, STARR used a suite of models to create the RI FIRMs, starting with the initial water levels (surge) estimated empirically using a statistical extreme value analysis at three buoys, Montauk,(CT), Newport and Providence (RI). This information was used to set the boundary and initial conditions of the Steady State Spectral Wave Model (STWAVE; Massey et al., 2011; Smith et al., 2001) to simulate waves traveling from deep water into the near shore region. Results of STWAVE were finally used as boundary conditions to propagate waves across the shoreline using a 1-D wave model, the Wave Height Analysis for Flood Insurance Studies (WHAFIS) developed in 1978 by the U.S. Army Corps of Engineers (FEMA, 1988). Since the WHAFIS model is a 1-D model, the inundation zones are estimated using linear spatial interpolation between transects. The method inherently creates issues since it assumes that bathymetry and topography are changing linearly between transects, while also neglecting wave energy focusing/defocusing effects due to refraction. The official FIRMs were updated in October 2013 for Southern Rhode Island (FEMA, 2012) .

In 2014 the Rhode Island Coastal Resources Management Council (CRMC) requested an independent evaluation of the 100-year storm's FIRMs. The University of Rhode Island (URI) responded to the request by applying a 2-D methodology referred to as the "NAST" method (NACCS-STWAVE; Grilli et al., 2016), to simulate the inundation zones based on the results of the NACCS study and the use of the 2-D wave model STWAVE to simulate wave propagation across the inundated areas. In the NACCS the USACE simulated about 1000 synthetic storms, both tropical and extra-tropical storms, along the East coast using the fully coupled surge and wave models ADCIRC (Luettich and Westerink, 2004)/STWAVE. Statistical spectral wave parameters, significant wave height and static water elevation, resulting from these simulations were recorded at 'save-points' scattered all along the East Coast expressed in terms of annual probability of exceedance. These results were then used as initial boundary conditions in the NAST method to simulate wave propagation in a high resolution grid (10m) across the shallow water coastal area and the inundation zone. The resulting NAST inundation maps showed significant differences with the current FIRM maps (Spaulding et al., 2016).

With the previous information under consideration, it can be concluded that there is much room for improvement on FEMA's maps. The method outlined by FEMA and executed by STARR is clearly outdated, with technological advancements allowing for more complicated and accurate models to be run on higher-resolution grids. One concern is based around the allowable models that FEMA has outlined, with no phase resolving models included, the physical processes of dynamic wave setup and run-up in the swash zone are completely missed in the development of FIRM's. Wave setup and run-up have been theoretically and observationally shown to greatly increase the inundation zone relative to that defined by storm surge only.

Evaluation of this process has usually been performed semi-empirically along selected 1-D transects (Stockdon et al., 2006). However only a phase resolving model can accurately simulate these processes in 2-D and currently their complexity and high computational time has limited their use. Kennedy et al., (2012) applied such a model (Demirbilek et al., 2009) in 1-D to the coastal area of Hawaii, as part of the United States Army Corps of Engineers Surge and Wave Island Modeling Studies (SWIMS). Runup was indeed found to be an extremely important component of the inundation in particular in a high slope environment such as Hawaii. More recently Li et al. (2014) used the Boussinesq Ocean and Surf Zone (BOSZ) model of Roeber and Cheung (2012a) in 2-D to similarly assess the inundation risk in Hawaii, reaching similar conclusions.

As a result of dynamic wave runup, additional forces resulting from high velocities may be produced in the swash zone that significantly increase the coastal hazard/community risk (Bender and Dean, 2005). For the purpose of this study, a 2-D phase resolving model (FUNWAVE) is used to simulate the 100-year storm, and results are compared to those of the FEMA approved phase averaged model STWAVE. This allows for a direct comparison of the influence of wave setup, swash, and run-up on overall inundation levels along the coast of Narragansett.

During extreme storms sediment erosion along coastal beaches can become a major problem, potentially leading to the breaching or complete destruction of dunes. When a dune loses its integrity it drastically changes the extent of flooding experienced behind it. For this reason it is important to map the extent of wave run-up for both an intact and eroded dune in areas that may be susceptible to dune breaching/flattening. In FEMA's protocol dunes are classified as subject to failure based on their overall sand reservoir ("540-square-foot" protocol), and they are accordingly, either assumed intact, fully removed, or partially truncated, before propagating waves across the inundated shoreline (Kevin Coulton et al., 2005). An alternative method was used in NACCS where a 100-year modified beach profile was assumed based on a semi-empirical approach (Grilli et al., 2016). Simulations performed on both natural and modified beach profiles, showed a significant increase in wave action behind modified dunes. This further confirms that the extent of wave runup can be significantly altered when dunes are eroded.

1.1.1 *Objective*

We propose to map the extent of wave runup and the associated impulse forces on the infrastructures for a "100-year storm", using a suite of state-of-the-art erosion and wave models. The coastal and onshore wave field is modeled using the phase resolving wave model FUNWAVE for two scenarios, (1) assuming a barrier beach system intact, and (2), assuming an eroded barrier beach system. The eroded dune profile is generated using the sediment erosion model, Extreme Beach Behavior (XBEACH) (Roelvink et al., 2009). XBeach simulations will show that a 100-year storm would significantly affect the dune system, flattening the dune, and significantly changing the flooding extent and the risk imposed on the coastal community. Results are compared with NAST results obtained using the phase averaged model STWAVE.

1.1.2 *Test site*

The test site, Narragansett, RI, with a particular focus on the Town Beach and surrounding historical buildings (Figure: 1.1) is selected for, (1) its history of significant damages during storm events inparticular during the 1938 hurricane (Holman and Sallenger, 1985; Island, 1938), (2), its societal importance as a vibrant dense local coastal community and (3), the presence of several historical buildings as part of the Narragansett's official Historical Area, in particular, the Coast Guard House, the “Towers”, the Post Office, the Dunes Club. Wave runup is recorded at each of these locations and results are compared for each simulation (Table: 1.11).

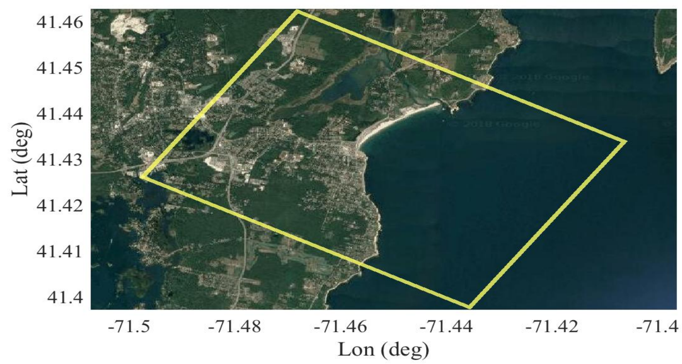

Fig. 1.1. Area of interest outlined for Narragansett Rhode Island.

1.2 Data

The topography and bathymetry data used for this study was created by merging NOAA’s digital elevation model (DEM) as the coastal bathymetry, combined with a land based DEM measured by an airborne LIDAR (April 22nd through May 6th, 2011; R.I. Geographic Information System (RIGIS) (Environmental Data Center, 2014)). The original resolution of the two data sets was 1/3 arc-sec (about 10 m), and 1 m, respectively. This combined DEM map was then interpolated to a 2 m resolution computational grid (Figure: 1.2). The DEM elevation map is referenced to the North American Vertical Datum of 1988 (NAVD 88) (Zilkoski et al., 2013).

The bottom friction was specified using a spatially variable Manning coefficient(n) based on landcover, as defined on Table 1.1, (Arcement and Schneider, 1989). The data was retrieved from RIGIS (RIGIS, 2015) with an original resolution of 30 m, interpolated on a 2 m resolution grid in the area of interest (Figure: 1.3).

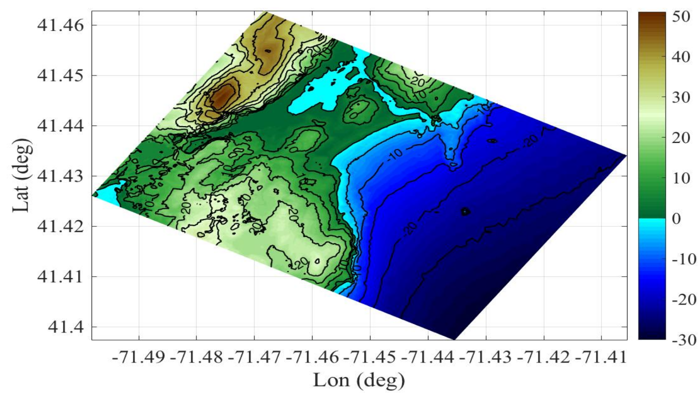

Fig. 1.2. Elevation map of Study Area, interpolated to 2 meter resolution. Color scale in meters. Data from (Environmental Data Center, 2014).

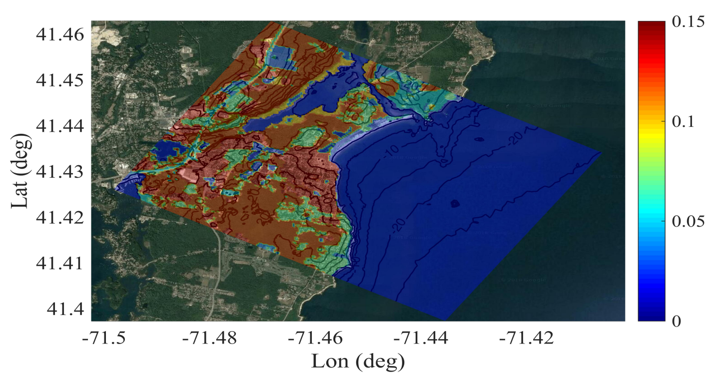

Fig. 1.3. Friction map of Study Area, defined by Manning Coefficient n (color scale: $s/m^{1/3}$) Data:(RIGIS, 2015).

Table 1.1. Manning bottom friction coefficient n ($s/m^{1/3}$) as a function of land type (Arcement and Schneider, 1989).

Land Category	Manning Coefficient n
Sandy Bottom (D_{50} = 0.4 mm)	0.02
Boulder/ Bare rock	0.04
Herbaceous Wetland	0.04
Shrubland	0.05
Mix Shrubland and Woody Wetlands	0.07
Woody Wetlands	0.1
Deciduous Forest	0.12
Mixed Forest	0.12
Evergreen Forest	0.15
Low Intensity Residential	0.07
High Intensity Residential	0.14
Roads	0.05

1.3 Methodology

A summary of the simulated numerical scenarios is presented in Table 1.2. In the first scenario, the 100-year storm is simulated using the fully non-linear phase resolving model FUNWAVE over the unchanged bathymetry/topography representing the current dune system. In the second scenario, the sediment erosion model XBeach is first used to simulate the post-storm beach and dune profile consistent with the "100-year" storm. The resulting XBeach elevation map is then used as initial condition to the wave propagation numerical simulation using FUNWAVE to map the extent of wave runup on the eroded dune system.

Finally, in a third scenario the 100-year storm is simulated over an assumed intact dune with STWAVE to assess the difference in predicted impact due to the use of a phase resolving rather than a phase averaged wave model.

A brief overview of each model as well as a definition of their computational grids and initial and boundary conditions is presented in the following subsections.

Table 1.2. Summary of the numerical scenarios.

Scenario	Model	Bathymetry/Topography
1	FUNWAVE	Original DEM
2 (a)	XBeach	Original DEM
2 (b)	FUNWAVE	DEM modified by XBeach results
3	STWAVE	Original DEM

1.3.1 *Shoreline morphology during 100-Year storm: modeling dune erosion*

The erosion model XBeach used in "surf-beat" mode was recently calibrated and validated for extreme storms at a similar site on the southern RI shoreline (Schambach et al., 2018). This mode was similarly successfully used in the literature for extreme events (Van Gent et al.(2008) test T4).

XBeach is a state-of-the-art open source 2-D horizontal numerical model developed to assess the natural coastal morphological response during time-varying storm conditions (Roelvink et al., 2009). The model has two hydrodynamic modules, a short wave and a depth-averaged flow module, as well as two morphodynamic modules, a morphology change and a sediment transport module. The model employs a phase-averaged description of wave groups and accompanying infra-gravity waves to resolve the swash dynamics. A roller model (Svendsen, 1984) is used to represent momentum stored in surface "rollers" leading to a shoreward shift in wave forcing. XBeach is applied to the nearshore zone to model the local beach and dune erosion. The model transports and redistributes sand, once eroded and suspended, according to the hydrodynamics associated with the wave field and the bathymetry, modified and updated in real time. A summary of the physics/equations involved in the XBeach model is presented in Harter and Figlus (2017). The Xbeach version Kingsday (v1.22.4867) was used for the purposes of this study (Deltares,).

Computational domain

XBeach's computational grid is defined in Table 1.3 and shown in Figure 1.4. The Cartesian grid extends about 6 km in the along-shore direction and 5 km in the cross-shore direction, while rotated to have the shoreline relatively parallel to the outer boundary of the domain. The grid spacing is variable with a minimum grid spacing set to (10 x 15) meters, in the cross- and along-shore directions respectively, as in Schambach et. al. (2018). The grid is rotated (θ) such that the main direction of propagation is perpendicular to the shoreline. Let us note that for computational purpose the grid is rotated 90 degrees clockwise so that the X axis is in the main direction of propagation.

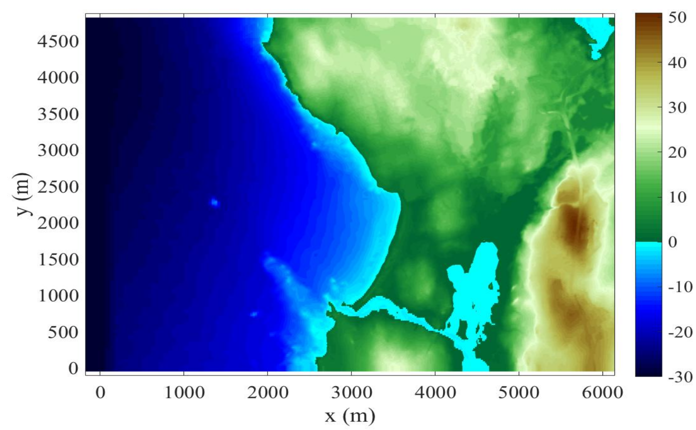

Fig. 1.4. XBeach Computational Elevation Map defined by NAVD88 datum. Coast line rotated to be aligned along eastern side of grid. (color scale: meters) (Environmental Data Center, 2014).

Table 1.3. XBeach Grid Parameters; origin(Xo,Yo), grid spacing (Dx/Dy), grid dimension (X Dim/ Y Dim), rotation angle (θ) defined positive in clockwise direction.

Xo (Lon)	Yo (Lat)	Dx (m)	Dy (m)	X:Dim (m)	Y:Dim (m)	θ (deg)	Friction
-71.4076	41.4340	10	15	6144	4784	-57	Variable Manning

XBeach model initial conditions

The bottom friction coefficient in XBeach is defined as spatially variable, with the Manning coefficient n value defined based on the land cover (Figure: 1.3; Table: 1.1). The non-sandy coastline outside the beach barrier dune system is defined as "non-erodible". This section of the shoreline is indeed formed of walls, buildings, paved areas, or large rocks (Figure 1.5).

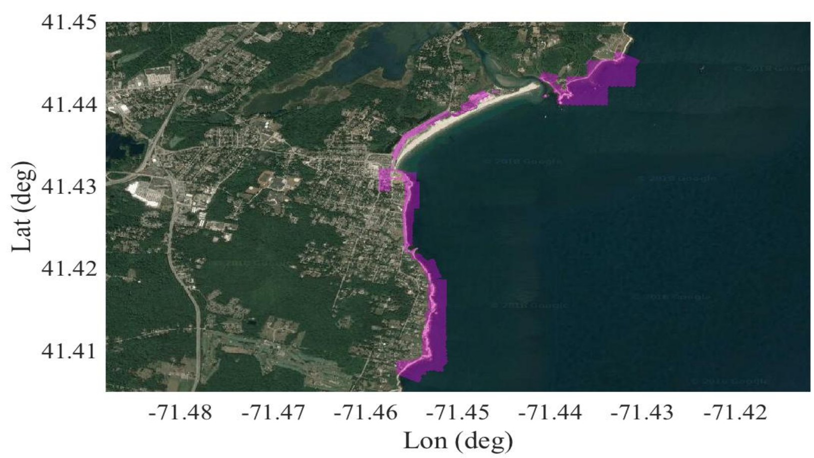

Fig. 1.5. XBeach Nonerodible Locations (rocks, walls, buildings, roads) (Google, 2018).

The choice of model parameter values is based on the calibration/validation performed by Schambach et. al. (2018). A complete list of the parameters and their assigned values used in these simulations is presented in Appendix (A.1).

XBeach model offshore boundary conditions

Similarly to Schambach et. al. (2018), the selected 100-year synthetic design storm is extracted from the NACCS database based on the similitude between the values of its spectral parameters and the values of the 100-year spectral parameters estimated using extreme value statistical analysis (Nadal-Caraballo et al., 2015). As a result, NACCS storm 4457 was selected, which extends over a 48-hour period (Cialone et al., 2015).

While the NACCS statistical analysis predicts at the grid off-shore boundary (Figure: 1.1) a significant wave height on the order of 7.5 to 8.0 m meters, with a Peak period on the order of 15.5 seconds, and a surge of 3.7 meters, storm 4457 predicts after 33 hours a significant waveheight on the order of 7.8 meters corresponding to a period of 15.0 seconds, with a peak period of 19 s occurring in the beginning of the storm; the maximum storm surge is 3.3 m. (Figures: 1.6 (a),(b),(c) respectively). The time series shown in these figures represents our selected 100-year SDS and was used as the offshore boundary conditions in XBeach, with a time discretization of 30 minutes for scenario 2 (a).

1.3.2 *Modeling inundation using phase-averaged wave model*

In scenario 3, the steady state phase-averaged wave model STWAVE version 6.0 was used to simulate wave propagation within the Narragansett Bay. STWAVE includes linear refraction, shoaling, wave breaking, and the redistribution of energy from wind to waves through non-linear wave-to-wave interactions to higher and lower frequencies (Hasselmann et al., 1973). The model does not include wave reflection, diffraction, or dynamic wave set-up. STWAVE uses TMA-spectral parameters to solve the wave action balance equation for wind generated gravity waves in water of finite depth (Hughes, 1984).

Computational Domain

STWAVE is used to propagate waves from deep water towards the coastal area of interest in a relatively large computational domain, with a fine resolution of 10m. The computational domain extends southerly towards Block Island (Figure 1.7) and covers 50 by 30 km (Table 1.4). A constant bottom friction was applied to the entire domain using a Manning coefficient $n = 0.02$, representative of an overall sandy bottom (Table 1.1).

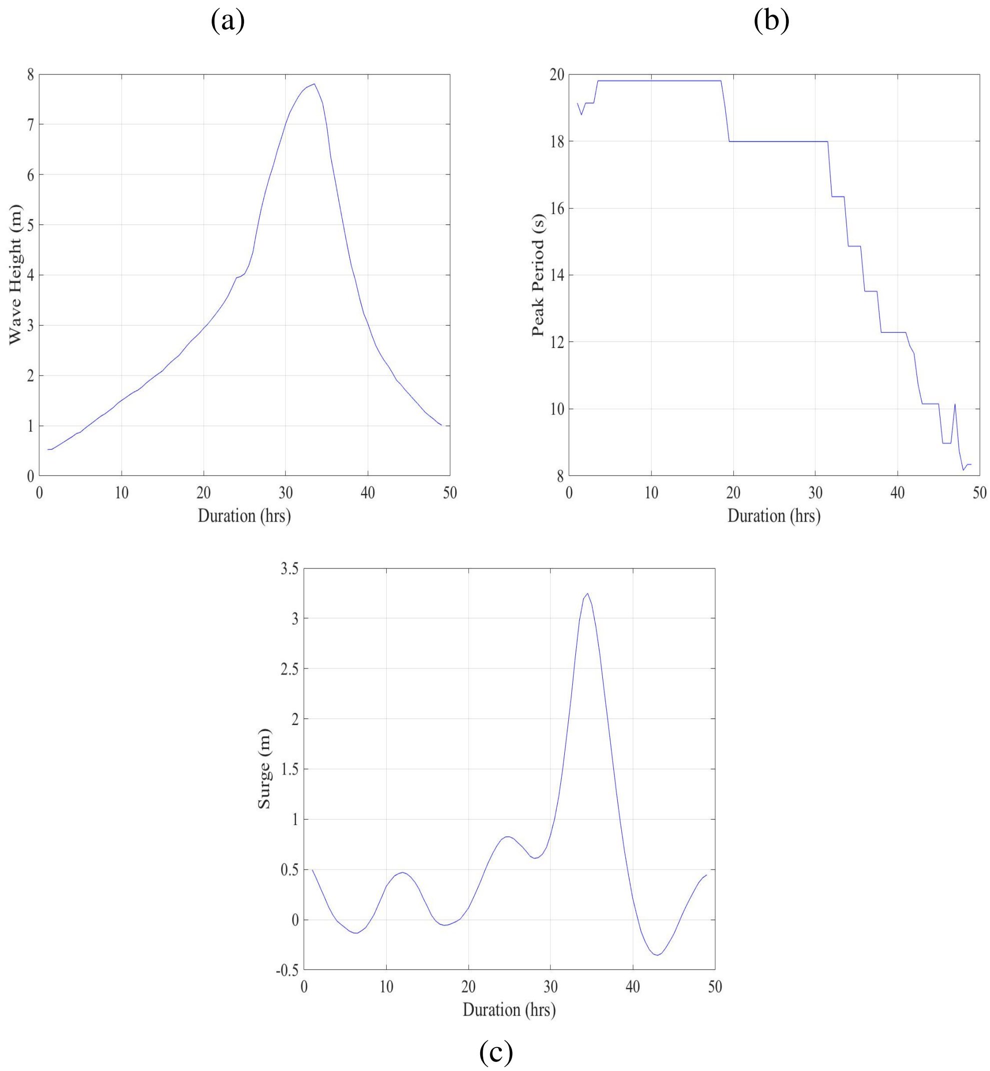

Fig. 1.6. NACCS data for storm 4457 in Narragansett Rhode Island (a) Significant Wave height (b) Peak Period (c) Storm Surge (Cialone et al., 2015).

Table 1.4. Large grid computational domains parameters used for wave propagation with STWAVE: origin (Xo/Yo), grid spacing (Dx/Dy), number of rows (Ni), number of columns (Nj), rotation angle (θ).

Xo (Lon)	Yo (Lat)	Dx/Dy (m)	Ni	Nj	θ (deg)	Friction
-71.1502	41.3057	10	4999	2999	0.0	Variable Manning

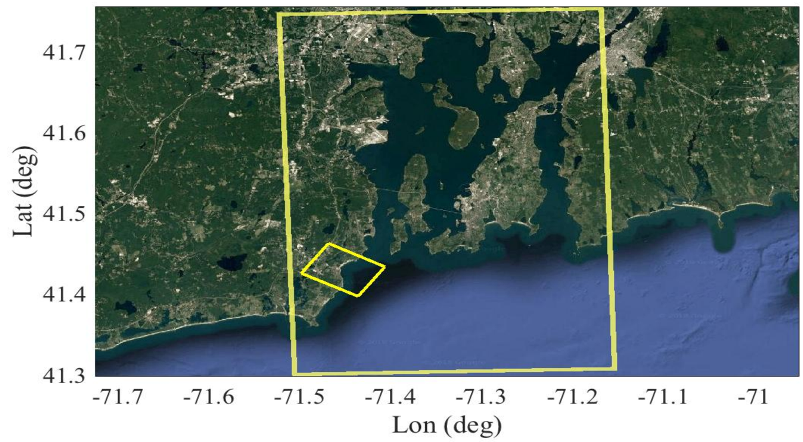

Fig. 1.7. STWAVE grid (large grid) and nested coastal grid (small grid) used to simulate waves for the 100-year storm using NACCS 's spectral parameters in boundary condition on the edge of the large grid.

Input parameters and boundary conditions

Offshore spectral boundary conditions are retrieved from the results of the NACCS (Cialone et al., 2015) which provides them at each save point for selected return periods (100-year in this scenario). Wind conditions are defined for the worse case scenario following the methodology presented in the NAST study (Grilli et al., 2017) . Offshore boundary conditions are summarized in Table 1.5.

Table 1.5. STWAVE input parameters as defined by the shallow water TMA spectrum, with the wind speed, wind direction, significant wave height (Hs), peak period (Tp), wave direction (α), and maximum surge.

Spectrum	Wind Sp. (m/s)	Wind Dir. (deg)	Hs (m)	Tp (sec)	α (deg)	Surge (m)
TMA	35	180	9	20	180	3.7

1.3.3 *Modeling inundation using phase-resolving wave model*

FUNWAVE is a FUlly-Non linear dispersive Boussinesq WAVE model, which includes refraction, diffraction and reflection, besides wave shoaling, breaking and dissipation. FUNWAVE was originally designed to solve the fully nonlinear Boussinesq wave equations for long waves such as swells or tsunamis in 1995 by (Wei et al., 1995). A full description of the latest model and equations is given in Shi et al., 2012.

The model is used in wave maker mode to simulate storm waves based on a TMA spectrum provided in offshore boundary condition. The wave generation theory at the base of the two-way numerical wavemaker is described in Wei et al. (1999). Wall boundary conditions are applied along edges of the domain parallel to the shoreline, while periodic boundary conditions are used along both lateral edges to ensure stability of the code. Sponge layers are placed behind the wavemaker in order to prevent reflected waves from re-reflecting behind the wave maker and reentering the wave field (both *direct sponge* and *friction sponges* are used). Initial parameters and boundary conditions are summarized in Table 1.8. The grid characteristics are summarized in Table 1.6.

Computational Domain

FUNWAVE's computational grid is a Cartesian grid covering the area shown on Figure 1.1, similar in extension and shape to the grid used in XBeach, but with a finer spatial discretization of 2 by 2 m. For computational purpose the grid is rotated 90 degrees clockwise to have the wave main direction of propagation parallel to the X-axis. In order for the lateral boundaries of the grid to satisfy the periodicity condition, the southern edge of the domain was replicated and flipped on the northern side (width 20% of the total width =956 meters). The boundary of the lateral periodicity region is highlighted in Figure 1.8 by a solid line. Characteristics of the grid are summarized in 1.6. Figure 1.8 (b), depicts the actual grid used for this simulation with a superimposed static surge level of 3.7 meters.

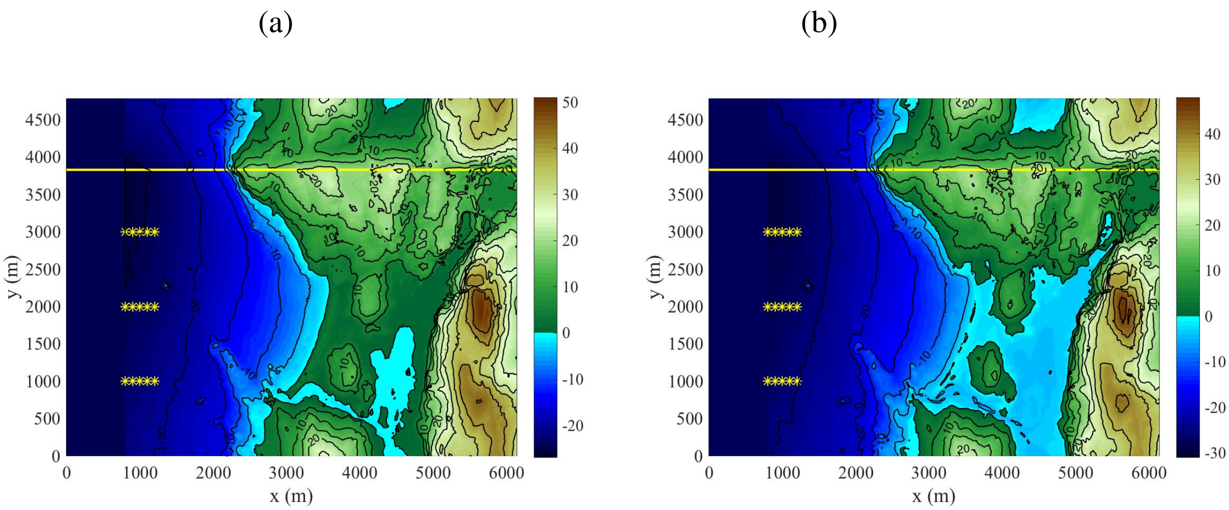

Fig. 1.8. FUNWAVE Computational Grid (a) DEM elevation map (b) DEM elevation with 3.7 m of surge. The solid line shows the limit of the the 'fake' lateral boundary used for periodic boundary conditions, the stars mark stations that were placed along 3 transects to test the wave maker (top to bottom: T1,T2,T3). Color Scale is in meters.

Table 1.6. FUNWAVE Grid Parameters. With its origin (Xo,Yo), grid spacing (Dx/Dy), x- and y-dimensions (mglob/nglob), and rotation angle (θ).

Xo (deg)	Yo (deg)	Dx,Dy (m)	mglob (m)	nglob (m)	θ (deg)	Friction
-71.4076	41.4340	2,2	6144	4784	-57	Variable Manning

Waves are generated with a numerical wave maker positioned at the offshore boundary of the domain. The area around the wave maker is flattened to constant depth (24.2 meters) to ensure numerical stability. The width of the flat region is estimated based on the peak wavelength (e.g., in water 24 m depth, the linear dispersion relationship implies that a wave train with a peak period of 15 seconds corresponds to a peak wavelength of about 220 m. A direct sponge layer at the offshore boundary is combined with a friction sponge with *Cd*= 10.0. The geometry of the offshore boundary is summarized in Table 1.7.

Table 1.7. FUNWAVE wave maker grid setup for Narragansett, Rhode Island.

Grid	Sponge layer width (m)	Wave maker position on X-axis	"Flat" wave maker width (from 0 in X-axis)
Narragansett	270 m	700 m	800 m

The bottom friction is spatially variable using a Manning coefficient *n* varying with the land coverage (Figure 1.3). The parts of the shoreline with large boulders or a wall, as along the Narragansett sea wall, are marked as *breakwaters* (Figure 1.9). Structures built with a foundation are marked as *obstacles* (Figure 1.10). Note that since we focus on the runup zone only the first three rows of houses are considered as *obstacles* (See appendix A.3, A.4).

Input parameters and boundary conditions

STWAVE simulations performed on the larger grid using NACCS save point data as input provide the spectral parameters necessary to define a TMA spectrum specified for input to FUNWAVE's irregular wavemaker at the offshore boundary of the coastal nested grid (significant waveheight and peak period). Input parameters are summarized in Table 1.8.

The NACCS database provides the initial storm surge value for the 100-year upper 95% confidence interval storm as used in the methodology described in more detail in

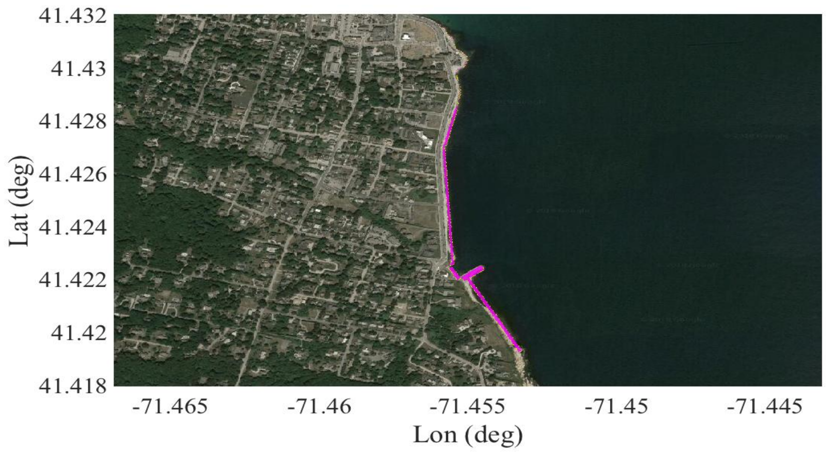

Fig. 1.9. FUNWAVE Breakwater locations for the DEM simulation have been highlighted on Google Earth (Google, 2018).

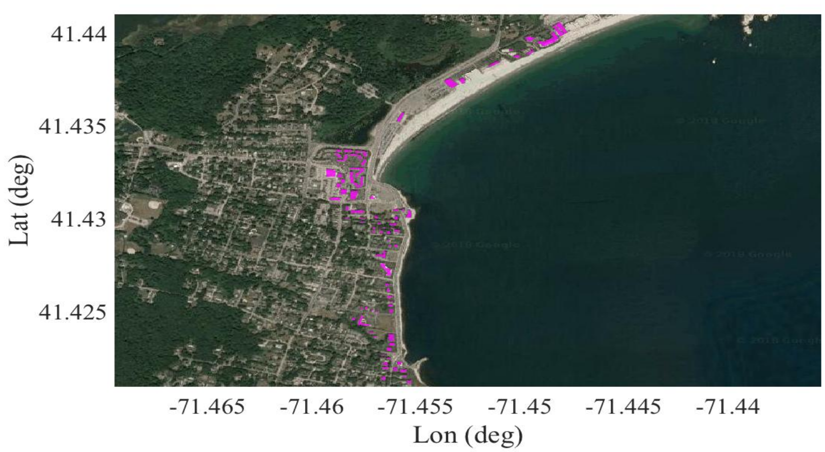

Fig. 1.10. FUNWAVE Obstacle locations have been highlighted on Google Earth (Google, 2018). Obstacle points identify spots on the grid that remain dry (building with foundations).

Table 1.8. Spectral parameters and initial storm surge level implemented on FUNWAVE irregular wave maker. The frequency range has been defined for incoming wave field based on the peak period (Tp), significant wave height (Hs), and depth.

Min Freq. (Hz)	Peak Freq. (Hz)	Max Freq. (Hz)	Hs (m)	Tp (sec)	Theta (deg)	Depth (m)	Surge (m)
0.0345	0.06	0.339	7.5	15.5	0	24.2	3.7

Grilli et al. (2017). The corresponding value at the edge of the offshore boundary of the nested grid is 3.7 m. A complete list of the model inputs is provided in the Appendix A.5. It must be mentioned that the values of the spectral parameters at the offshore edge of the nested grid resulting from the wave simulations using STWAVE for the 100-year storm on the large grid are in agreement with NACCS' values for these parameters at the same location (within 0.5 meters at 'center' location, Table 1.9). Our large grid has a resolution of 10 m, while the NACCS wave grid had a resolution of 200 m.

The adequacy of the wave maker to simulate the wave train corresponding to the spectral parameters provided as input is assessed using numerical wave gauges located along the x-axis (X = 800,900,1000 ,1100,1200 m) and y-axis (Y= 1000,2000,3000 m).

1.4 Results

1.4.1 *Dune erosion*

The new topography resulting from dune erosion and sand transport predicted by XBeach both seaward and landward is shown in Figure 1.11. Relative changes of elevation as compared to the initial topography are shown on Figure 1.12 and Figure 1.13, showing area experiencing erosion and deposition respectively. A considerable amount of erosion (dune flattened by 3 to 5 m) occurs along the dune face, especially on the eastern side of the domain, by the mouth of the river.

1.4.2 *Nested grid boundary conditions*

Spectral parameters used as offshore initial and boundary conditions at the offshore boundary of the nested grid (Table 1.9) are obtained using STWAVE to simulate the

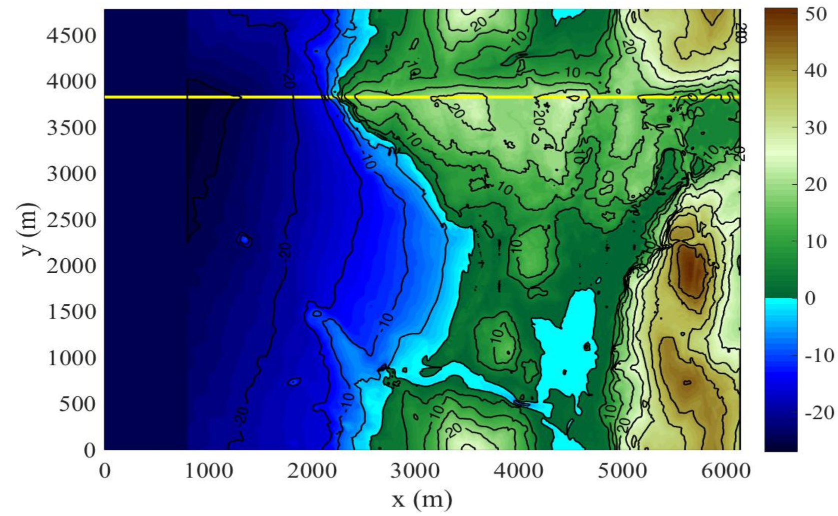

Fig. 1.11. XBeach results for sediment transport, post storm bathymetry/topography (color scale: meters). The periodicity region has been marked with a solid line.

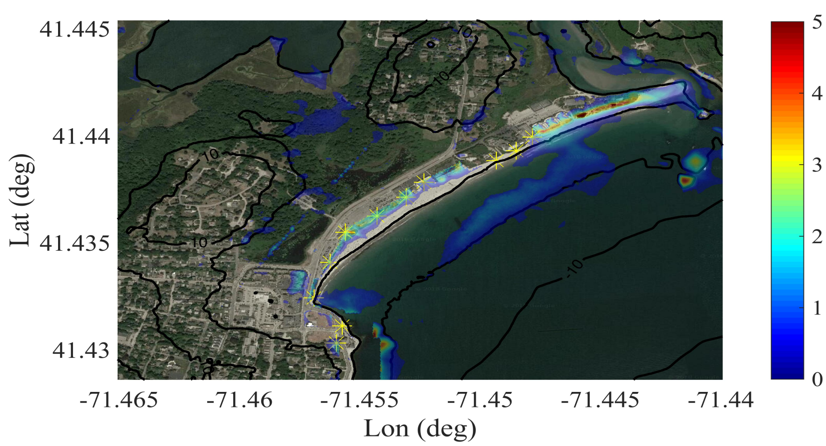

Fig. 1.12. XBeach results for sediment *erosion*, positive values depict a decrease in elevation relative to the original DEM grid, data from (Environmental Data Center, 2014). Contour lines depict original DEM levels spaced at 5 m intervals, the asterisks mark 11 key locations used for model comparisons. Data is displayed on Google Earth (Google, 2018) (color scale: meters).

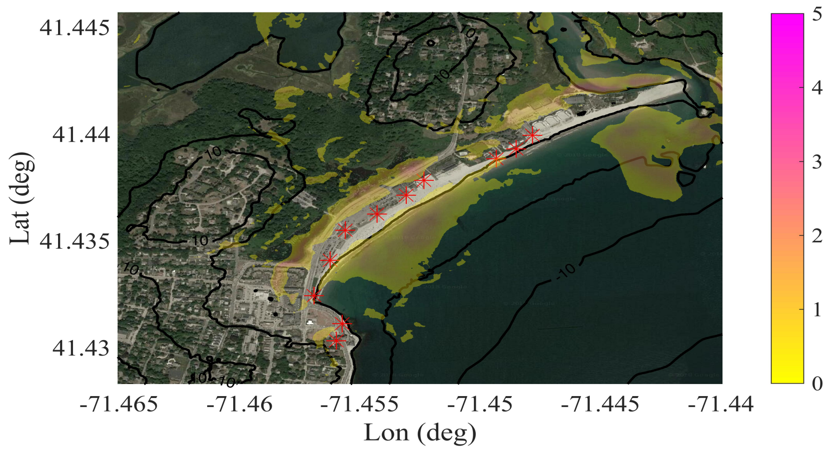

Fig. 1.13. XBeach results for sediment *deposition*, positive values depict an increase in elevation relative to the original DEM grid, data from (Environmental Data Center, 2014). Contour lines depict original DEM levels spaced at 5 m intervals, the asterisks mark 11 key locations used for model comparisons. Displayed on Google Earth (Google, 2018) (color scale: meters).

wave propagation on a high resolution grid from trusted NACCS' save points.

Table 1.9. STWAVE results for spectral parameters; significant wave height (Hs), and peak period (Tp) at three locations along the offshore boundary.

	Lon (deg)	Lat (deg)	Hs (m)	Tp (sec)
West	-71.4335	41.3988	7.5	15.3
Center	-71.4198	41.4166	7.5	15.4
East	-71.4064	41.4331	8.0	15.3

Figure 1.14 focus on the significant wave heights simulated with STWAVE in the area of interest surrounding the Narragansett Town Beach. These results are used to compare to the values calculated with FUNWAVE. Figure 1.14 shows that in STWAVE waves do not overtop a large portion of the healthy dune behind Narragansett Town Beach. While flooding still ensues around the face of the dunes, it should be noted that certain areas remain dry.

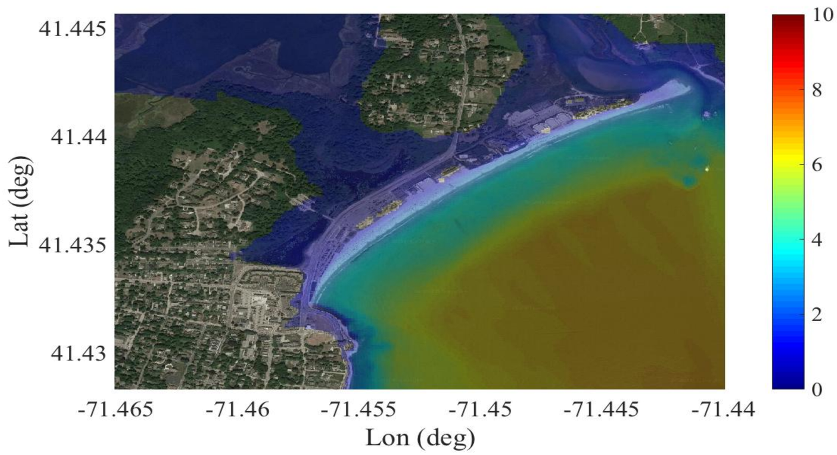

Fig. 1.14. STWAVE results for significant wave height (Narragansett Town Beach, R.I). A close up view of results in the area of interest, note that dune tops are 'dry'. Data is displayed on Google Earth (Google, 2018) (color Scale: meters).

1.4.3 *Inundation using FUNWAVE*

The spectral verification at the wave gauge stations located onshore of the wave maker confirms that the input spectrum is indeed initially well reconstructed (Figure 1.8). This verification is performed using both a zero-crossing method to estimate the significant wave height, H_s, and a P-welch spectral analysis to estimate analytically the spectral energy density and H_{mo} ($H_{mo} \cong H_s$) as a function of the zero-order moment of the spectrum (m_o ; $H_{mo} = 4\sqrt{m_o}$). This equation holds true in deep water for Rayleigh distributed waves, which is why here (in intermediate water) results differ from the directly measured significant wave height performed using zero-crossing method. Results (Table 1.10) show that the spectral energy intended to be create is indeed generated relatively accurately (5 % underestimation) by the wave maker as shown by results in station 1; both methods are in good agreement with slight differences ($\tilde{5}$%) between H_s and H_{mo} due to wave non-linearity. Complete simulation time is 11,000 seconds (corresponding to 1300 waves estimated from zero-up crossing).

Table 1.10. FUNWAVE irregular wave-maker validation: H_s and H_{mo} at the three transects, T1,T2,T3 (each, 5 stations (*Sta*)) 100 meters apart (Figure 1.8); calculated using Welch's power density spectrum (*PW*), and the zero-up-crossing method (*ZUC*), respectively.

	Sta: 1	Sta: 2	Sta: 3	Sta: 4	Sta: 5
T1: PW	7.02	7.13	6.36	6.53	5.89
T1: ZUC	6.79	6.85	6.01	6.15	5.80
T2: PW	7.82	6.49	5.91	6.62	7.08
T2: ZUC	7.60	6.40	5.69	6.36	6.77
T3: PW	6.40	6.96	6.98	6.78	7.62
T3: ZUC	6.05	6.56	6.65	6.33	7.47

Figure 1.15 shows the envelope of maximum water level (η) (above NAVD88) throughout the entire simulation. Locations where surface elevations were predicted to be greater as a result of dune erosion can be seen in Figure 1.16. Figure 1.17 shows similar results but relative to ground elevation, showing the flow depth. Locations where the flow depth was predicted to be increased as a result of sediment erosion can be seen in Figure 1.18. Furthermore, flow depths have been depicted in the swash zone alone (Figure 1.19), which highlights the influence of dynamic wave setup. These figures show both of the FUNWAVE scenarios placed side-by-side so that a direct comparison can be seen for a healthy dune and eroded dune system.

The corresponding maximum impulse forces experienced at each location on the grid are shown in Figure 1.20, depicting the eastern end of Narragansett Town Beach. A closer view of the forces acting the buildings themselves can be seen in Figures 1.22, and 1.23. The impulse force (F_i) (Equation 1.4.3), is the force caused by the water flow acting on an imaginary wall of unit width perpendicular to the flow. It is usually expressed in kilo-Newton (kN/m). The maximum impulse force is calculated at each grid cell as a function of the maximum velocity, u, water depth, h, and water density as;

$$F_i = \rho * h * u^2$$

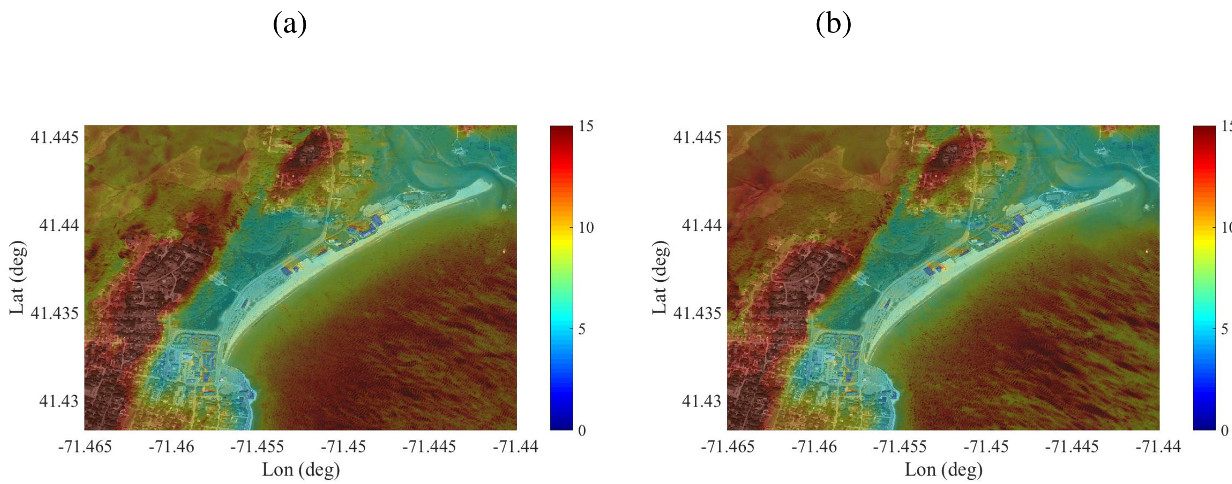

Fig. 1.15. Envelope of maximum surface elevations (m) in FUNWAVE simulations (referred to NAVD88) for: (a) scenario 1 (dune intact), (b) scenario 2 (dune eroded).

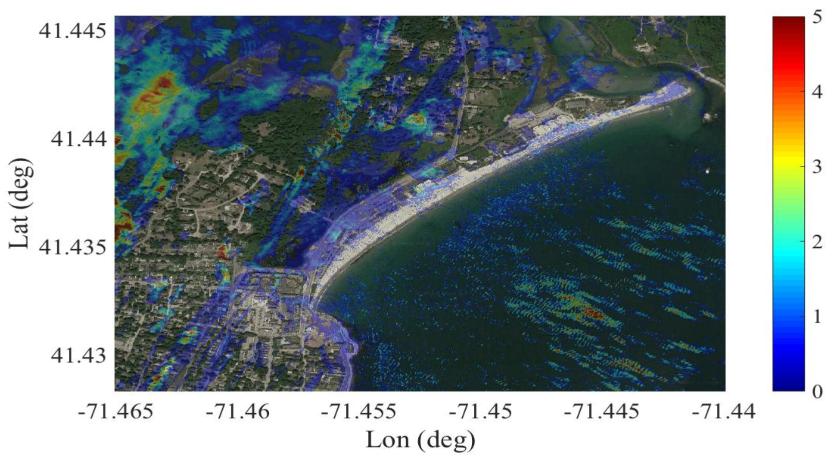

Fig. 1.16. Difference in maximum surface elevations (m) from FUNWAVE simulations (referred to NAVD88). Eroded > Intact: found by subtracting scenario 1 (dune intact) from scenario 2 (eroded dune).

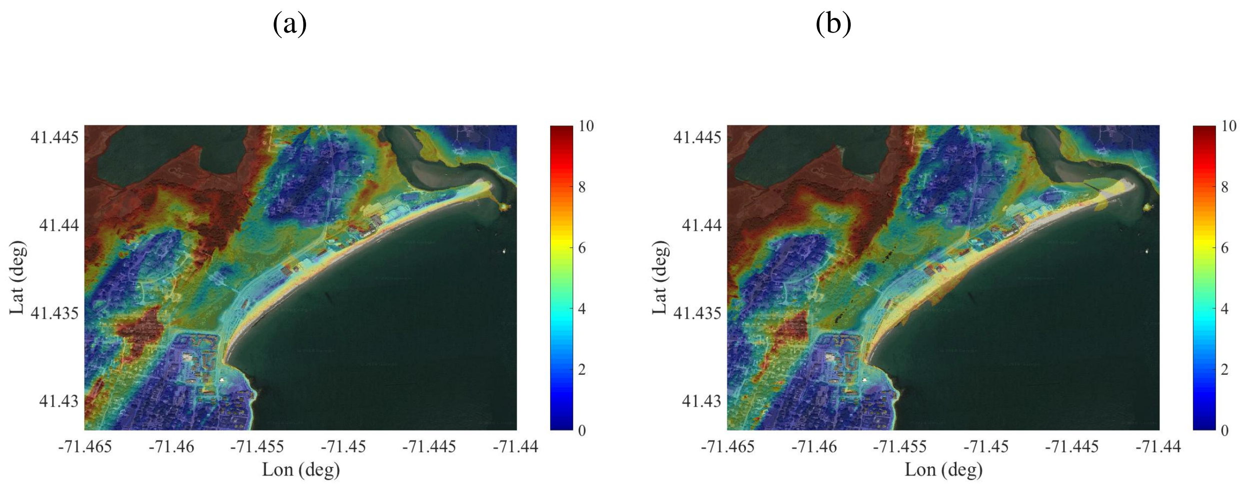

Fig. 1.17. Maximum flow depths (m) from FUNWAVE simulations for: (a) scenario 1 (dune intact), (b) scenario 2 (eroded dune).

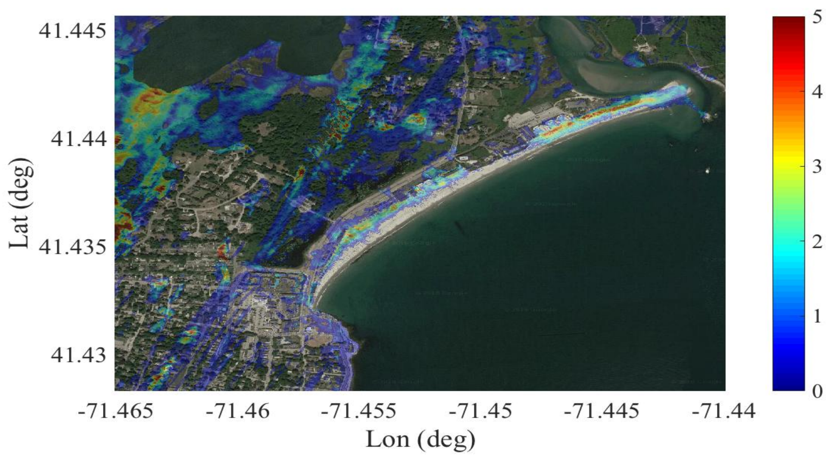

Fig. 1.18. Difference in maximum flow depths (m) from FUNWAVE simulations (referred to NAVD88). Eroded > Intact: found by subtracting scenario 1 (dune intact) from scenario 2 (eroded dune).

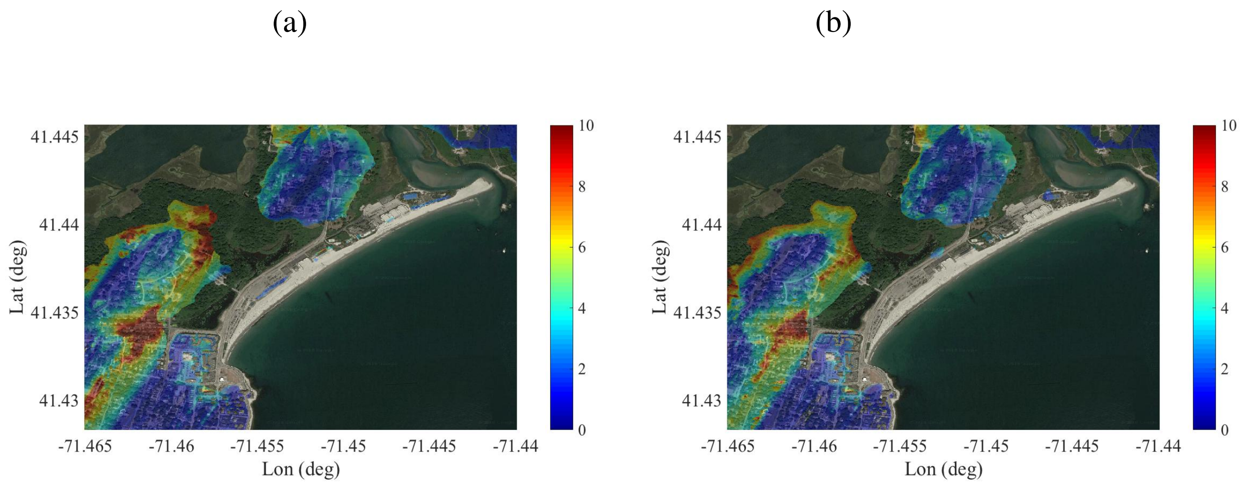

Fig. 1.19. Maximum flow depths (m) in the swash zone (above static surge = 3.7 m) from FUNWAVE simulations for: (a) scenario 1 (dune intact), (b) scenario 2 (eroded dune).

Comparison of the maximum impulse force assuming an eroded coast line rather than an intact coastline shows (Figure 1.21) that larger impulse forces occur in the nearshore area. Indeed, the erosion creates deeper inundated areas in many coastal locations, resulting in a potentially larger increase impulse force acting on coastal structures. However, the sand transported offshore protects the shoreline in an alternative way, by reducing locally the offshore depth and consequently inducing more offshore wave breaking and energy dissipation. In this simulation, however, the increase in flooding does compensate for the larger offshore wave breaking and the structures located on the shoreline experience a larger impulse force (especially along the eastern end of the beach). Table 1.12 shows the maximum impulse forces that occurred at each save point for the two FUNWAVE scenarios (intact dune and eroded dune, respectively). The eroded dune scenario surprisingly had a decrease in impulse forces at 5 of the stations (P1,P2,P4,P9,P11), while only two stations showed a significant increase (P7,P8).

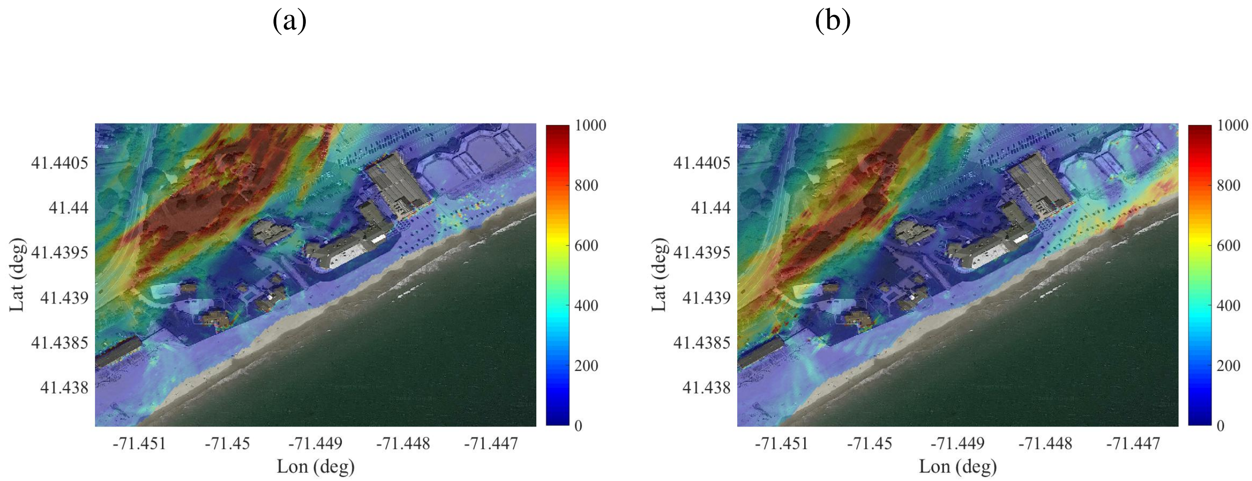

Fig. 1.20. Maximum impulse forces (kN/m) at the Dunes Club and eastern end of Narragansett town beach estimated from FUNWAVE simulations for: (a) scenario 1 (dune intact) (b) scenario 2 (eroded dune).

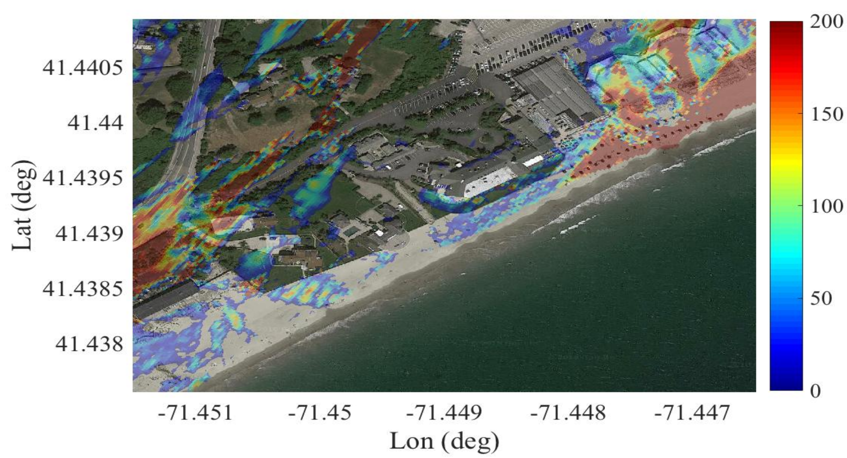

Fig. 1.21. Difference in maximum impulse forces (kN/m) at the Dunes Club and eastern end of Narragansett town beach estimated from FUNWAVE by subtracting scenario 1 (dune intact) from scenario 2 (eroded dune).

(a) (b)

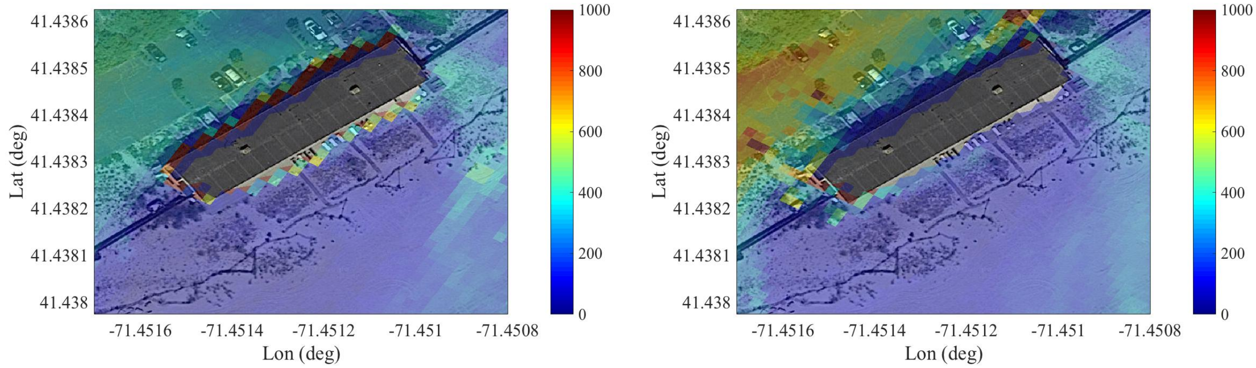

Fig. 1.22. Maximum impulse forces (kN/m) on Condo's along Narragansett beach from FUNWAVE simulations for: (a) scenario 1 (intact dune), (b) scenario 2 (eroded dune).

(a) (b)

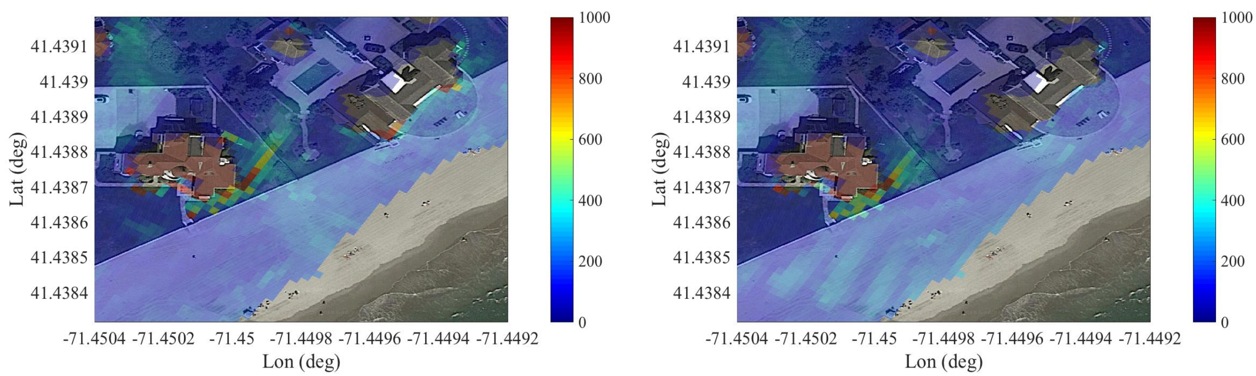

Fig. 1.23. Maximum impulse forces (kN/m) on two houses along Narragansett beach from FUNWAVE simulations for: (a) scenario 1 (intact dune), (b) scenario 2 (eroded dune).

1.4.4 *Runup at critical save points*

Results for the 3 scenarios (Table 1.2) are compared at stations located at eleven key locations stretching across the Narragansett Town Beach area (Table 1.11) and are shown in Figure 1.24.

Wave height and impulse force evaluation

Table 1.11 shows a comparison of the predicted significant wave heights (H_s) at each save point for each scenario. For scenario 1, at each critical save point FUNWAVE almost systematically predicts a larger significant wave height than STWAVE on the order of 43% (average), which results from the ability of FUNWAVE to capture the dynamic wave set-up and better simulate large individual waves. There is a significant spatial variability, for example, Point 3 shows nearly identical results, while Point 9 shows 2.83 m of additional wave height, signaling that this location is much more sensitive to dynamic wave set-up and runup.

Fig. 1.24. Eleven save points are marked by asterisks. The four asterisks with rectangular box's mark locations used for wave runup empirical calculations based on Stockdon et. al. (2006).

Table 1.11. Significant wave heights compared at 11 key points for each simulation including STWAVE, FUNWAVE scenario 1 and 2 (*FW* dune intact and eroded, respectively)

Label	Description	Lon (deg)	Lat (deg)	Depth (m)	STW (m)	FW Intact (m)	FW Eroded (m)
P1	C. Guard House	-71.4560	41.4303	-1.36	0.0	0.98	1.41
P2	Post Office	-71.4557	41.4311	-0.94	0.59	2.50	2.51
P3	Condos	-71.4569	41.4324	-1.73	2.16	2.10	2.37
P4	Beach Parking	-71.4562	41.4341	-1.17	1.35	1.60	1.97
P5	Ticket Office	-71.4556	41.4355	-0.81	0.33	1.84	2.62
P6	Dune Top	-71.4543	41.4363	0.03	0.16	1.30	1.75
P7	Concessions	-71.4531	41.4371	-0.94	0.66	2.41	2.35
P8	Cabanas (Stilts)	-71.4478	41.4399	-0.94	1.13	1.74	2.27
P9	House	-71.4523	41.4378	-2.80	0.70	3.53	3.25
P10	Dunes Club 1	-71.4493	41.4388	-2.52	2.18	3.52	3.77
P11	Dunes Club 2	-71.4485	41.4393	-1.56	1.94	2.94	4.04

Table 1.12. Impulse forces, F_{i} (kN) compared at 11 key locations for FUNWAVE scenario 1 and 2 (dune intact and eroded, respectively)

	F_{i} Intact dune	F_{i} Eroded dune
P1	252	205
P2	163	138
P3	490	517
P4	226	113
P5	117	128
P6	55	66
P7	377	417
P8	428	764
P9	321	184
P10	194	197
P11	425	402

Wave runup evaluation

Results from scenario 1 (FUNWAVE, assuming an intact dune), and 3 (STWAVE) are compared to wave runup empirical calculations (Eqn. 1.4.4) as defined by Stockdon et. al. (2012). Please refer to the Appendix for details of the variables involved in Stockdon's wave runup equations (A.10). N_{98} refers to the maximum wave runup experienced during a storm based on the 2% probability of exeedence. Stockdon's empirical formulation expresses N_{98} as a function of the deep water wave height (H_0), wave length (L_0), and beach slope (βm) as,

$$\eta_{98} = \eta_{50} + (1.1) + (S/2)$$

$$\eta_{50} = \eta_{tide} + \eta_{surge} + \eta_{setup}$$

$$\eta_{setup} = 0.35 * \beta_m * (H_0 L_0)^{1/2}$$

$$S = [H_0 L_0 (0.563\beta_m^2 \pm 0.005)]^{1/2}$$

Stockdon's formulation is applicable for a dune environment with no coastal obstructions (e.g., buildings, walls). Four of the eleven selected save points qualify to apply Stockdon's formulation for wave runup (P4,P5,P6,P8). One-dimensional transects were created for

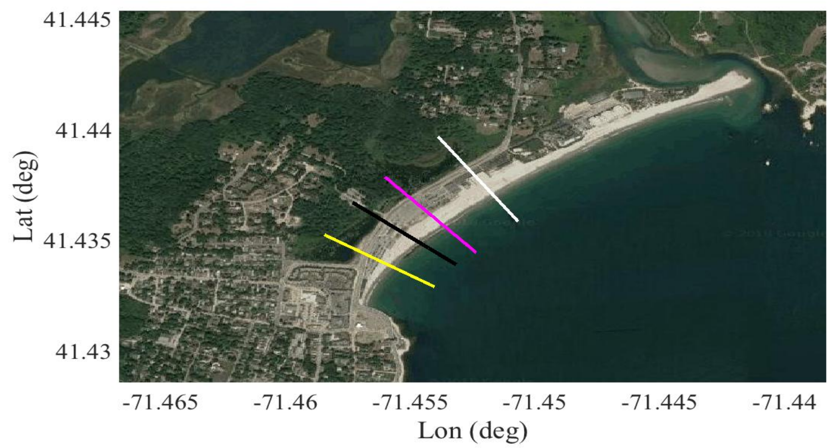

Fig. 1.25. Transect locations selected for empirical wave runup calculations as defined by Stockdon et. al. (2012). From left to right, transects 1,2,3, and 4, corresponding to 'save points' (4,5,6, and 8, respectively) in Table 1.11.

each of these points extending 125 m perpendicular to the coastline in both the onshore and offshore directions (total of 250 m)(Figure 1.25).

Table 1.13 presents at transect the runup estimated using FUNWAVE and Stockdon's formulation. (N_{98}) for FUNWAVE simulations is calculated using the mean value of the top 2% of the maximum surface elevations, combined with the static surge level (3.7 m). This is compared with runup estimations using STWAVE results and theory of random (linear) waves. Indeed, to assess the runup from scenario 3, we assume from linear wave theory and random wave theory that waves are Rayleigh distributed. Then, the maximum surface elevation can be defined as ($\eta_{\max} = 1.3\ H_s$) which, when combined with the static surge (3.7 m) provides an upper bound estimation of the wave runup. Results are shown in Table 1.13, Stockdon's results are in good agreement with FUNWAVE, with FUNWAVE's predictions falling within 0.22 meters of the empirical Stockdon calculations for all but one transect (T4), for which FUNWAVE predicts an additional 0.8 meters. (Stockdon et al., 2012)

Table 1.13. Wave runup (m) estimated using Stockdon's formulation (Stockdon et. al., 2012) FUNWAVE (dune intact) and STWAVE along 4 transects across Narragansett Town Beach (Figure 1.25).

Transect	η_{50} **Stockdon**	η_{98} **STWAVE**	η_{98} **Stockdon**	η_{98} **FUNWAVE**
T1	3.96	5.46	6.02	6.24
T2	3.93	4.13	6.02	6.21
T3	3.85	3.91	5.93	6.0
T4	3.92	5.17	6.01	6.85

Figure 1.26 shows a cross section at each transect. While offshore surface elevations are relatively consistent between the two models (FUNWAVE and STWAVE), one can see that STWAVE surface elevations abruptly decrease nearly to the static water level when waves pass the dune crest, while FUNWAVE's values are decreasing more progressively.

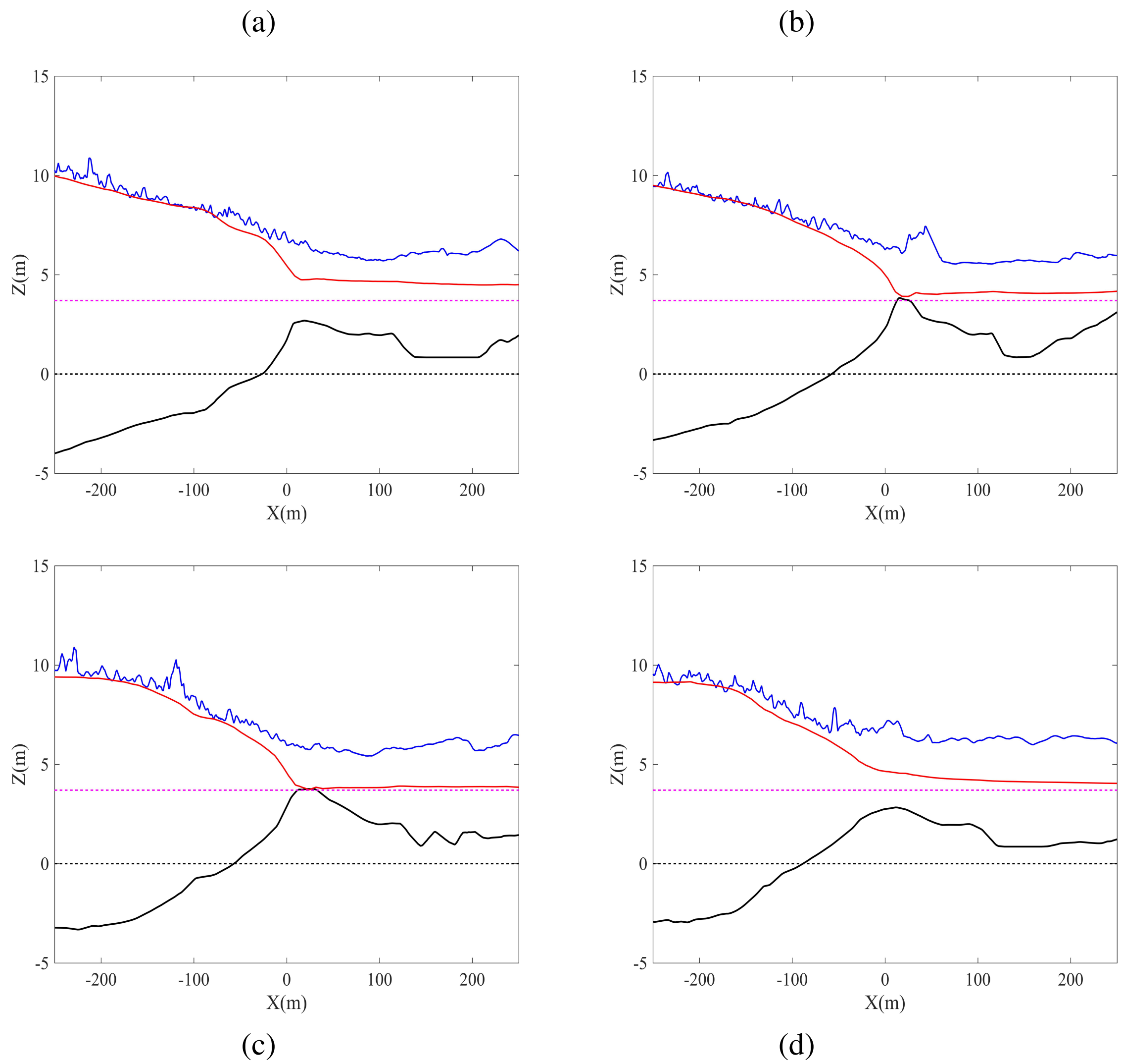

Fig. 1.26. Transect data (a) T1, (b) T2, (c) T3, (d) T4. Maximum surface elevations (η_{max}) are displayed for FUNWAVE (blue line), and STWAVE (red line), with the original DEM bathymetry/topography (black line). The static surge level = 3.7 m (dashed pink line), and NAVD88 z=0 (black dashed line).

1.5 Conclusion

A large portion of damage and loss of human life that occurs during major coastal storms is from the impacts of water. For this reason it is absolutely crucial to provide the most accurate predictions for inundation including, storm surge but also predicted wave elevation and current. Yet FEMA's currently approved wave-modeling guidelines in RI permit only phase-averaged models. This introduces the inherent problem that dynamic wave setup is completely missed from FEMA's predictions. For this reason the phase resolving model FUNWAVE was used to compare results to FEMA's approved model STWAVE in order to highlight the importance of including dynamic wave setup.

When analyzing results from Table 1.11 it was found that there was a mean increase in significant wave height of 1.21 m between all 11 points when comparing STWAVE to the FUNWAVE-DEM simulation. This value increased further to 1.56 m when the influence of sediment erosion/deposition was considered by relating STWAVE to the FUNWAVE-XBeach simulation. The greatest increase occurred at Point 9 with a value of 2.83 m and 2.55 m respectively for each simulation. This increase is the direct result of dynamic wave runup, as Point 9 was placed just behind the semi-circular wall protecting one of the large houses on Narragansett Beach. A phase-averaged model cannot predict this process. Indeed, by definition a phase-averaged model does not capture this short of time scale event, surf-beats (minutes) and runup, at the scale of an individual wave, and consequently misses a significant part of the hazard affecting the coastline. Wave reflection also is neglected which can locally enhance waves near structures.

Empirical calculations for wave runup based on Stockdon's (2012) formulations agree very well with FUNWAVE's predictions doing transects for the western end of the beach, providing support in the model validation for this specific type of hazard (storm) and spatial scale. Three of the four transects used to measure wave runup fell within 0.2 meters of the empirical calculations, while an additional 0.8 meters was predicted for the fourth transect by FUNWAVE. At the opposite, runup "rough" estimations based on STWAVE predictions underpredicted wave runup by 0.6, 1.9, 2.0 and 0.8 meters respectively for each of the four transects.

Results show that the phase-averaged wave model STWAVE as compared to the phase resolving wave model FUNWAVE under-predicts both significant wave height and maximum water elevations. These conclusions should be taken into consideration in the future in order to better prepare for the devastating effects of 100-year storms on our sandy coastlines.

List of References

Arcement, G. J. and Schneider, V. R. (1989). Guide for selecting manning's roughness coefficients for natural channels and flood plains.

Battjes, J. A. (1974). *Computation of set-up, longshore currents, run-up and overtopping due to wind-generated waves*. PhD thesis, TU Delft, Delft University of Technology.

Bender, C. J. and Dean, R. G. (2005). Wave transformation by axisymmetric three-dimensional bathymetric anomalies with gradual transitions in depth. *Coastal engineering*, 52(4):331–351.

Cialone, M. A., Massey, T. C., Anderson, M. E., Grzegorzewski, A. S., Jensen, R. E., Cialone, A., Mark, D. J., Pevey, K. C., Gunkel, B. L., and McAlpin, T. O. (2015). North atlantic coast comprehensive study (naccs) coastal storm model simulations: Waves and water levels. Technical report, ENGINEER RESEARCH AND DEVELOPMENT CENTER VICKSBURG MS COASTAL AND HYDRAULICS LAB.

Deltares. Xbeach. [Online]. Available: https://oss.deltares.nl/web/xbeach/download.

Demirbilek, Z., Nwogu, O. G., Ward, D. L., and Sánchez, A. (2009). Wave transformation over reefs: Evaluation of one-dimensional numerical models. Technical report, ENGINEER RESEARCH AND DEVELOPMENT CENTER VICKSBURG MS COASTAL AND HYDRAULICS LAB.

Environmental Data Center, U. o. R. I. (2014). Digital elevation model, dem11. [Online]. Available: http://www.rigis.org/pages/2014-usgs-lidar-dem.

FEMA (1988). Wave height analysis for flood insurance studies. Technical report, Federal Emergency Management Agency.

FEMA (2012). Summary report of coastal engineering analyses, dfirm update for coastal analysis for washington county, ri; task order 1: Coastal hazard analysis. Technical report, Federal Emergency Management Agency.

FEMA (2016). Guidance for flood risk analysis and mapping.

Google (2018). Google earth. [Online]. Available: https://www.google.com/earth/.

Grilli, A., Spaulding, M. L., Oakley, B. A., and Damon, C. (2017). Mapping the coastal risk for the next century, including sea level rise and changes in the coastline: application to charlestown ri, usa. *Natural Hazards*, 88(1):389–414.

Grilli, A. R., Spauding, M. L., Schambach, L., Smith, J., and Bryant, M. (2016). Comparing inundation maps developed using whafis and stwave: A case study in washington county, ri. *Earth and Space*, page 147.

Guza, R. and Thornton, E. B. (1982). Swash oscillations on a natural beach. *Journal of Geophysical Research: Oceans*, 87(C1):483–491.

Hasselmann, K., Barnett, T., Bouws, E., Carlson, H., Cartwright, D., Enke, K., Ewing, J., Gienapp, H., Hasselmann, D., Kruseman, P., et al. (1973). Measurements of wind-wave growth and swell decay during the joint north sea wave project (jonswap). *Ergänzungsheft 8-12*.

Holman, R. A. and Sallenger, A. (1985). Setup and swash on a natural beach. *Journal of Geophysical Research: Oceans*, 90(C1):945–953.

Hughes, S. A. (1984). The tma shallow-water spectrum description and applications. Technical report, Coastal Engineering Research Center Vicksburg MS.

Island, R. (1938). Hurricane of 1938 aftermath in narragansett. [Online]. Available: http://sos.ri.gov/virtualarchives/items/show/290.

Jensen, R., Cialone, A., Smith, J., Bryant, M., and Hesser, T. (2016). Regional wave modeling and evaluation for the north atlantic coast comprehensive study. *Journal of Waterway, Port, Coastal, and Ocean Engineering*, 143(2):B4016001.

Kevin Coulton, P., Dean, C. B., Hatheway, D., Honeycutt, C. M., Johnson, J., Jones, P. C., and Komar, P. P. (2005). Fema coastal flood hazard analysis and mapping guidelines focused study report. Technical report, Federal Emergency Management Agency.

Kirby, J. T., Wei, G., Chen, Q., Kennedy, A. B., and Dalrymple, R. A. (1998). Funwave 1.0: fully nonlinear boussinesq wave model-documentation and user's manual. *research report NO. CACR-98-06*.

Knutson, T. R., McBride, J. L., Chan, J., Emanuel, K., Holland, G., Landsea, C., Held, I., Kossin, J. P., Srivastava, A., and Sugi, M. (2010). Tropical cyclones and climate change. *Nature Geoscience*, 3(3):157.

Longuet-Higgins, M. S. and Stewart, R. (1964). Radiation stresses in water waves; a physical discussion, with applications. In *Deep Sea Research and Oceanographic Abstracts*, volume 11, pages 529–562. Elsevier.

Luettich, R. A. and Westerink, J. J. (2004). *Formulation and numerical implementation of the 2D/3D ADCIRC finite element model version 44. XX*. R. Luettich.

Nadal-Caraballo, N. C., Melby, J. A., and Gonzalez, V. M. (2015). Statistical analysis of historical extreme water levels for the us north atlantic coast using monte carlo life-cycle simulation. *Journal of Coastal Research*, 32(1):35–45.

Nielsen, P. and Hanslow, D. J. (1991). Wave runup distributions on natural beaches. *Journal of Coastal Research*, pages 1139–1152.

RIGIS (2015). Rhode island land use and land cover 2011.

Roelvink, D., Reniers, A., Van Dongeren, A., de Vries, J. v. T., McCall, R., and Lescinski, J. (2009). Modelling storm impacts on beaches, dunes and barrier islands. *Coastal engineering*, 56(11-12):1133–1152.

Schäffer, H. A. and Svendsen, I. A. (1989). Surf beat generation on a mild-slope beach. In *Coastal Engineering 1988*, pages 1058–1072.

Schambach, L., Grilli, A. R., Grilli, S. T., Hashemi, M. R., and King, J. W. (2018). Assessing the impact of extreme storms on barrier beaches along the atlantic coastline: Application to the southern rhode island coast. *Coastal Engineering*, 133:26–42.

Spaulding, M. L., Grilli, A., Damon, C., Crean, T., Fugate, G., Oakley, B. A., and Stempel, P. (2016). Stormtools: coastal environmental risk index (ceri). *Journal of Marine Science and Engineering*, 4(3):54.

Stockdon, K. S. D. H. F., Sopkin, D. S. T. K. S., and Sallenger, N. G. P. A. H. (2012). National assessment of hurricane-induced coastal erosion hazards: Gulf of mexico. *US Geological Survey*.

Svendsen, I. A. (1984). Mass flux and undertow in a surf zone. *Coastal Engineering*, 8(4):347–365.

Wei, G., Kirby, J. T., Grilli, S. T., and Subramanya, R. (1995). A fully nonlinear boussinesq model for surface waves. part 1. highly nonlinear unsteady waves. *Journal of Fluid Mechanics*, 294:71–92.

Zilkoski, D., Richards, J., and Young, G. (2013). Results of the general adjustment of the north american vertical datum of 1988. am congr surv mapp surv land inf syst 52 (3): 133–149.

APPENDIX

Appendix

A.1 XBeach Params.txt

XBeach Params.txt as defined by Schambach et al. 2018

General

tidelen = 98

D50 = 0.00058

D90 = 0.00131

struct = 1

nelayer = nebed.dep

bedfriction = manning

bedfricfile = bedfricfile.txt

facua = 0.3

eps = 0.05

morfac = 10

Grid parameters

depfile = bed.dep

posdwn = 0

nx = 883

ny = 570

alfa = 0

vardx = 1

xfile = x.grd

yfile = y.grd

xori = 0

yori = 0

thetamin = 225

thetamax = 315

dtheta = 90

thetanaut = 1

Model time

tstop = 172800

Tide boundary conditions

zs0file = tide.txt

tideloc = 2

Wave boundary condition parameters

instat = jons

Wave-spectrum boundary condition parameters

bcfile = filelist.txt

Output Variables

tintg = 900

outputformat = fortran

A.2 STWAVE Grid Schematic

Coordinate system angle: defined in degrees, zero pointing along the positive x-axis increasing counterclockwise.

A.3 FUNWAVE: Obstacle File

Definition of FUNWAVE *obstacle* file, the reason for including.

The obstacle file option in FUNWAVE denotes areas within the domain that will stay 'dry' forever, making it impossible for water to pass through or over. Hence, along the coastline any structures built with a foundation were marked as an obstacle (Figure

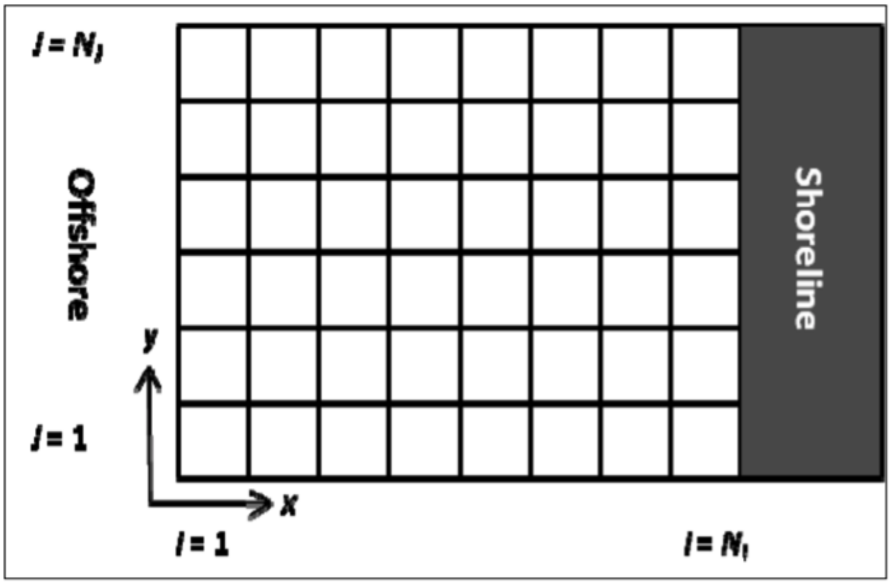

Fig. A.1. STWAVE Grid Schematic.

1.10). Due to the high density of urban development along the western side of domain, only the first three rows of houses were marked as obstacles.

A.4 FUNWAVE: Breakwater File

Definition of FUNWAVE *breakwater* file, the reason for including.

A breakwater file can also be used that artificially adds dissipation through the use of a sponge layer in locations that may have a sharp depth gradient as the result of rocks/breakwater. Figure 1.9 marks the areas within the domain of interest that were included in the breakwater file, adding dissipation along the Narragansett sea wall and surrounding rocks.

A.5 FUNWAVE: Input File *input.txt*

Copy of FUNWAVE *input.txt* file used for simulation in Narragansett, Rhode Island.

!INPUT FILE FOR BOUSS TVD

HOT START = F

FileNumber HOTSTART = 1

PX = 16

PY = 8

DEPTH TYPE = DATA

DEPTH FILE = Narrbathy2m.txt

WaterLevel = 3.7

DepthFormat = ELE

DEPTH FLAT = 24.21

SLP = 0.05

Xslp = 10.0

Mglob = 3072

Nglob = 2392

TOTAL TIME = 15500.0

PLOT INTV = 200.0

PLOT INTV$_{S}TATION$ = 0.5

SCREEN INTV = 1.0

HOTSTART INTV = 360000000000.0

StretchGrid = F

Lon West = 120.0

Lat South = 0.0

Dphi = 0.0042

Dtheta = 0.0042

T INTV mean = 50.0

STEADY TIME = 100.0

DX = 2.0

DY = 2.0

INI UVZ = F

ETA FILE = z.txt

U FILE = u.txt

V FILE = v.txt

WAVEMAKER = WK$_IRR$

NumWaveComp = 1505

PeakPeriod = 15.5

AMP = 1.0

DEP = 0.78

LAGTIME = 5.0

XWAVEMAKER = 400.0

Xc = 501.00

Yc = 501.00

WID = 100.0

Time ramp = 80.0

Delta WK = 0.5 ! width parameter 0.3-0.6

DEP WK = 24.21

Xc WK = 700.0

Tperiod = 15.5

AMP WK = 0.0232

Theta WK = 0.0

FreqPeak = 0.0662

FreqMin = 0.0345

FreqMax = 0.3388

Hmo = 10.6

GammaTMA = 3.3

ThetaPeak = 0.0

Sigma Theta = 0.0

FRICTION SPONGE = T

DIFFUSION SPONGE = F

DIRECT SPONGE = T

Sponge west width = 270.0

Sponge east width = 0.0

Sponge south width = 0.0

Spongenorth width = 0.0

R sponge = 0.85

A sponge = 5.0

CDsponge = 10.0

OBSTACLE FILE= NarrObstacleFull.txt

BREAKWATER FILE = NarrBreakFull.txt

DISPERSION = T

Gamma1 = 1.0

Gamma2 = 1.0

Gamma3 = 1.0

Beta ref = -0.531

SWE ETA$_{D}EP$ = 0.80

Friction Matrix = T

Cd file = Narr$_{f}ric_{2}m.txt$

Time Scheme = Runge$_{K}utta$

HIGH ORDER = FOURTH

CONSTRUCTION = HLL

CFL = 0.5

FroudeCap = 3.0

MinDepth = 0.1

MinDepthFrc = 0.1

SHOW BREAKING = F

Cbrk1 = 0.65

Cbrk2 = 0.35

T INTV mean = 20.0

C smg = 0.25

NumberStations = 107

STATIONS FILE = stationNarrFinal.txt

FIELD IO TYPE = BINARY

DEPTH OUT = T

U = F

V = F

ETA = T

Hmax = T

Hmin = F

MFmax = F

Umax = F

VORmax = F

Umean = F

Vmean =F

ETAmean = F

MASK = T

MASK9 = F

SXL = F

SXR = F

SYL = F

SYR = F

SourceX = F

SourceY = F

P = F

Q = F

Fx = F

Fy = F

Gx = F

Gy = F

AGE = F

TMP = F

WaveHeight = F

A.6 STWAVE Results Narragansett Bay

A.7 FUNWAVE: Irregular Wavemaker

For this paper the irregular wave maker was used with initial input parameters for waves defined by the TMA shallow-water spectrum, which will be combined with a wrapped-normal directional-spreading function to simulate a directional sea state (Shi, 2017). In the model, the initial input spectrum is divided into 1000 frequency components and then redistributed into a user-specified number of components with equal energy. The wave maker source function technique is then implemented on each frequency bin.

Directionally, the main axis of the wavemaker is aligned with the y-axis, propagating waves along the x-axis towards the shoreline. Post simulation calculations can be made on spectral simulations with the understanding that the average and root-mean-square wave heights are calculated at each grid point using the zero-crossing method. The significant wave (H_s) height will be calculated using Goda's findings (Goda et. al.

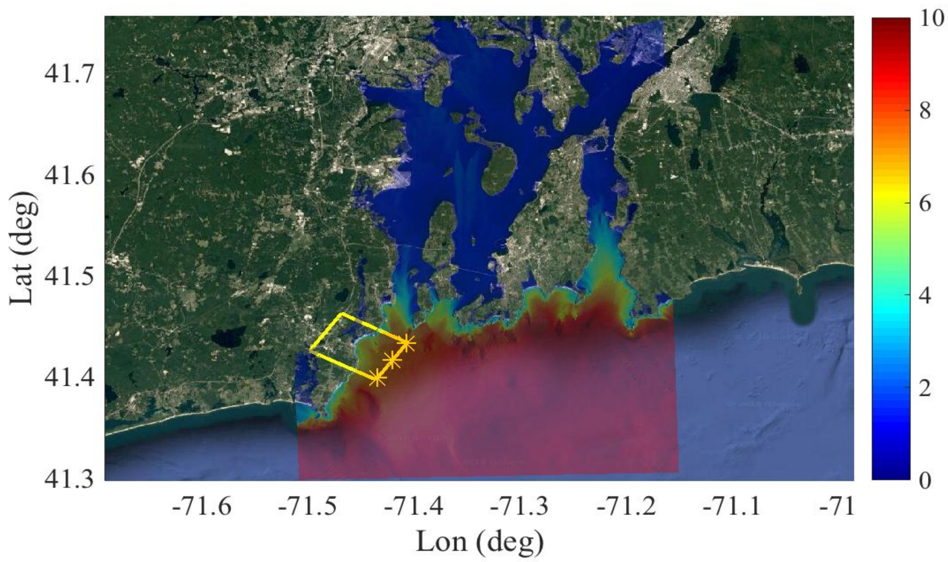

Fig. A.2. STWAVE results for significant wave height (Narragansett Bay, R.I). The FUNWAVE domain has been outlined, with the three input locations marked as stars along the outer boundary (Table 1.9). Data is displayed on Google Earth (color scale: meters).

2010).

$$H_{1/3} = H_s = 4.004\sqrt{m_0}$$

With m_0 representing the time averaged surface elevation (η) squared over one period:

$$m_0 = \frac{1}{t_2 - t_1}\int_{t_1}^{t_2} \eta^2 dt$$

This can be viewed as the area beneath the curve formed by the TMA spectral density plot. The m_0 value will play the most important role when comparing theoretical predictions to actual model results, using it to solve for the significant wave height (H_s).

A.8 FUNWAVE: Wavemaker Timeseries

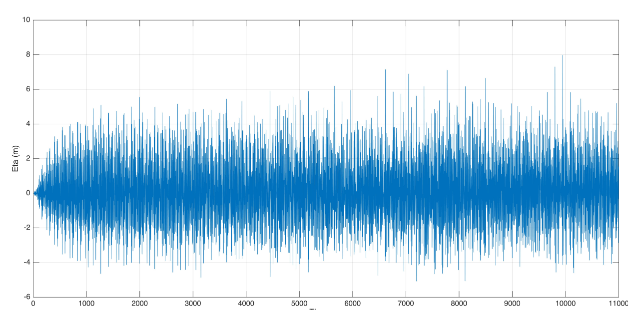

Fig. A.3. Time series of surface elevations (*eta* meters) from Transect one, station 1. Data collected at 0.1 second intervals over a total of 11,000 seconds.

Table A.1. FUNWAVE irregular wave-maker validation for XBeach post grid simulation. Significant wave heights are presented for three transects (T1,T2,T3) consisting of 5 stations (*Sta*) each separated by 100 meters (visually represented in Figure 1.8). *Hs* values were calculated at each station using both Welch's power density spectrum (*PWelch*), and the zero-up-crossing method (*ZUC*)

	Sta: 1	Sta: 2	Sta: 3	Sta: 4	Sta: 5
T1: PWelch	6.71	6.71	6.06	6.33	4.93
T1: ZUC	6.40	6.73	5.78	6.03	4.73
T2: PWelch	7.56	6.22	5.41	6.47	6.85
T2: ZUC	7.44	6.23	5.31	6.22	6.71
T3: PWelch	6.03	6.51	6.81	6.52	6.94
T3: ZUC	5.73	6.12	6.34	6.16	6.72

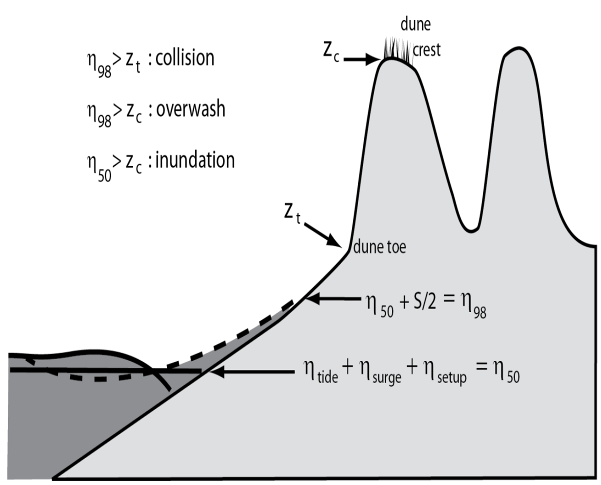

Fig. A.4. "Sketch defining the relevant morphological and hydrodynamic parameters in the storm impact scaling model of Sallenger (2000) (modified from Stockdon and other, 2009)." (Stockdon et. al., 2012)

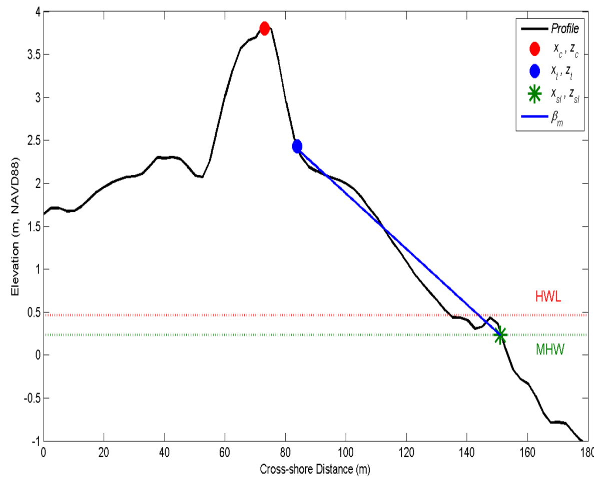

Fig. A.5. "Cross-shore profile of lidar-based elevations indicating the locations of the dune crest (x_c,z_c), toe (x_t,z_t), shoreline (x_{sl},z_{sl}), mean beach slope (β_m), mean high water (MHW), and high water line (HWL). Abbreviation: m, meter." (Stockdon et. al., 2012

A.9 FUNWAVE scenario two: Irregular Wavemaker Validation

A.10 Stockdon Wave runup definitions

A.11 Stockdon beach slope definitions

A.12 Impulse force equations

$$F_i = \rho * h * u^2$$

$$u = \sqrt{u_{vel}^2 + v_{vel}^2}$$

$$h = \eta - h$$

BIBLIOGRAPHY

Arcement, G. J. and Schneider, V. R., "Guide for selecting manning's roughness coefficients for natural channels and flood plains," 1989.

Battjes, J. A., "Computation of set-up, longshore currents, run-up and overtopping due to wind-generated waves," Ph.D. dissertation, TU Delft, Delft University of Technology, 1974.

Bender, C. J. and Dean, R. G., "Wave transformation by axisymmetric three-dimensional bathymetric anomalies with gradual transitions in depth," *Coastal engineering*, vol. 52, no. 4, pp. 331–351, 2005.

Cialone, M. A., Massey, T. C., Anderson, M. E., Grzegorzewski, A. S., Jensen, R. E., Cialone, A., Mark, D. J., Pevey, K. C., Gunkel, B. L., and McAlpin, T. O., "North atlantic coast comprehensive study (naccs) coastal storm model simulations: Waves and water levels," ENGINEER RESEARCH AND DEVELOPMENT CENTER VICKSBURG MS COASTAL AND HYDRAULICS LAB, Tech. Rep., 2015.

Deltares. "Xbeach." [Online]. Available: https://oss.deltares.nl/web/xbeach/download

Demirbilek, Z., Nwogu, O. G., Ward, D. L., and Sánchez, A., "Wave transformation over reefs: Evaluation of one-dimensional numerical models," ENGINEER RESEARCH AND DEVELOPMENT CENTER VICKSBURG MS COASTAL AND HYDRAULICS LAB, Tech. Rep., 2009.

Environmental Data Center, U. o. R. I. "Digital elevation model, dem11." 2014. [Online]. Available: http://www.rigis.org/pages/2014-usgs-lidar-dem

FEMA, "Wave height analysis for flood insurance studies," Federal Emergency Management Agency, Tech. Rep., 1988.

FEMA, "Summary report of coastal engineering analyses, dfirm update for coastal analysis for washington county, ri; task order 1: Coastal hazard analysis." Federal Emergency Management Agency, Tech. Rep., 2012.

FEMA. "Guidance for flood risk analysis and mapping." 2016. [Online]. Available: https://www.fema.gov/media-library-data/1487006131257-2845d429eb63ddd109e9ba1d3ed026d5/FIRM_Database_Guidance_May_2016.pdf

Google. "Google earth." 2018. [Online]. Available: https://www.google.com/earth/

Grilli, A., Spaulding, M. L., Oakley, B. A., and Damon, C., "Mapping the coastal risk for the next century, including sea level rise and changes in the coastline: application to charlestown ri, usa," *Natural Hazards*, vol. 88, no. 1, pp. 389–414, 2017.

Grilli, A. R., Spauding, M. L., Schambach, L., Smith, J., and Bryant, M., “Comparing inundation maps developed using whafis and stwave: A case study in washington county, ri,” *Earth and Space*, p. 147, 2016.

Guza, R. and Thornton, E. B., “Swash oscillations on a natural beach,” *Journal of Geophysical Research: Oceans*, vol. 87, no. C1, pp. 483–491, 1982.

Hasselmann, K., Barnett, T., Bouws, E., Carlson, H., Cartwright, D., Enke, K., Ewing, J., Gienapp, H., Hasselmann, D., Kruseman, P., *et al.*, “Measurements of wind-wave growth and swell decay during the joint north sea wave project (jonswap),” *Ergänzungsheft 8-12*, 1973.

Holman, R. A. and Sallenger, A., “Setup and swash on a natural beach,” *Journal of Geophysical Research: Oceans*, vol. 90, no. C1, pp. 945–953, 1985.

Hughes, S. A., “The tma shallow-water spectrum description and applications,” Coastal Engineering Research Center Vicksburg MS, Tech. Rep., 1984.

Island, R. “Hurricane of 1938 aftermath in narragansett.” 1938. [Online]. Available: http://sos.ri.gov/virtualarchives/items/show/290

Jensen, R., Cialone, A., Smith, J., Bryant, M., and Hesser, T., “Regional wave modeling and evaluation for the north atlantic coast comprehensive study,” *Journal of Waterway, Port, Coastal, and Ocean Engineering*, vol. 143, no. 2, p. B4016001, 2016.

Kevin Coulton, P., Dean, C. B., Hatheway, D., Honeycutt, C. M., Johnson, J., Jones, P. C., and Komar, P. P., “Fema coastal flood hazard analysis and mapping guidelines focused study report,” Federal Emergency Management Agency, Tech. Rep., 2005.

Kirby, J. T., Wei, G., Chen, Q., Kennedy, A. B., and Dalrymple, R. A., “Funwave 1.0: fully nonlinear boussinesq wave model-documentation and user’s manual,” *research report NO. CACR-98-06*, 1998.

Knutson, T. R., McBride, J. L., Chan, J., Emanuel, K., Holland, G., Landsea, C., Held, I., Kossin, J. P., Srivastava, A., and Sugi, M., “Tropical cyclones and climate change,” *Nature Geoscience*, vol. 3, no. 3, p. 157, 2010.

Longuet-Higgins, M. S. and Stewart, R., “Radiation stresses in water waves; a physical discussion, with applications,” in *Deep Sea Research and Oceanographic Abstracts*, vol. 11, no. 4. Elsevier, 1964, pp. 529–562.

Luettich, R. A. and Westerink, J. J., *Formulation and numerical implementation of the 2D/3D ADCIRC finite element model version 44. XX*. R. Luettich, 2004.

Nadal-Caraballo, N. C., Melby, J. A., and Gonzalez, V. M., “Statistical analysis of historical extreme water levels for the us north atlantic coast using monte carlo life-cycle simulation,” *Journal of Coastal Research*, vol. 32, no. 1, pp. 35–45, 2015.

Nielsen, P. and Hanslow, D. J., “Wave runup distributions on natural beaches,” *Journal of Coastal Research*, pp. 1139–1152, 1991.

RIGIS. “Rhode island land use and land cover 2011.” 2015. [Online]. Available: http://www.edc.uri.edu/rigis

Roelvink, D., Reniers, A., Van Dongeren, A., de Vries, J. v. T., McCall, R., and Lescinski, J., “Modelling storm impacts on beaches, dunes and barrier islands,” *Coastal engineering*, vol. 56, no. 11-12, pp. 1133–1152, 2009.

Schäffer, H. A. and Svendsen, I. A., “Surf beat generation on a mild-slope beach,” in *Coastal Engineering 1988*, 1989, pp. 1058–1072.

Schambach, L., Grilli, A. R., Grilli, S. T., Hashemi, M. R., and King, J. W., “Assessing the impact of extreme storms on barrier beaches along the atlantic coastline: Application to the southern rhode island coast,” *Coastal Engineering*, vol. 133, pp. 26–42, 2018.

Spaulding, M. L., Grilli, A., Damon, C., Crean, T., Fugate, G., Oakley, B. A., and Stempel, P., “Stormtools: coastal environmental risk index (ceri),” *Journal of Marine Science and Engineering*, vol. 4, no. 3, p. 54, 2016.

Stockdon, K. S. D. H. F., Sopkin, D. S. T. K. S., and Sallenger, N. G. P. A. H., “National assessment of hurricane-induced coastal erosion hazards: Gulf of mexico,” *US Geological Survey*, 2012.

Svendsen, I. A., “Mass flux and undertow in a surf zone,” *Coastal Engineering*, vol. 8, no. 4, pp. 347–365, 1984.

Wei, G., Kirby, J. T., Grilli, S. T., and Subramanya, R., “A fully nonlinear boussinesq model for surface waves. part 1. highly nonlinear unsteady waves,” *Journal of Fluid Mechanics*, vol. 294, pp. 71–92, 1995.

Zilkoski, D., Richards, J., and Young, G., “Results of the general adjustment of the north american vertical datum of 1988. am congr surv mapp surv land inf syst 52 (3): 133–149,” 2013.